Development of a geochemical model to predict leachate water quality associated with coal mining practices

KN van Zweel

20706391

Dissertation submitted in fulfilment of the requirements for the degree *Magister Scientiae* in Environmental Sciences (specialising in Hydrology and Geohydrology) at the Potchefstroom Campus of the North-West University

Supervisor: Dr SR Dennis

May 2015

Summary

South Africa mines coal to supply in the growing energy demands of the country. A majority of these mines are opencast resulting in back filled pits and above ground disposal facilities. Leachate emanating from these disposal sites are saline and in most cases highly acidic. Currently the standard testing procedure to quantify expected leachate qualities include Acid Base Accounting (ABA), Net-acid Generating test (NAG), static-and kinetic leaching.

The aim of this study is to model standard humidity cell leach tests performed using the PHREEQC code. This model can then be scaled up to field conditions to model 1D reactive transport. It is commonly accepted that the rate of pyrite oxidation in backfilled pits and waste storage facilities is governed by the rate of oxygen ingress and that no pyrite oxidation take place in the saturated zone. This is not the case for humidity cells, as sufficient oxygen is available for reaction. Pyrite reactions rates in humidity cells is expected to be governed by a combination of available reaction surface and ash layer resistance. This is modelled in PHREEQC (Parkhurst & Appelo, 2003) using the KINETIC block. Leachate composition is then modelled in the column by making use of the TRANSPORT block. The experimental data is fitted by using the reactive surface and ash layer diffusion coefficient as a fitting parameter.

PHREEQC does not have a gas transport module to model oxygen diffusion through the column. Due to this shortfall of PHREEQC, the influence of oxygen ingress in the system can not be directly modelled under kinetic conditions. Davis and Ritchie (1986a) proposed an anlylitical solution in which the integrated sulphate production rate can be calculated for a waste heap dump. This rate takes into account the influence of oxygen ingress and the development of an ash layer resistance to the pyrite oxydation rate. This intergrated rate can then be defined in a RATES block in PHREEQC.

The Aproximate Analytical Solution (AAS) model proposed by Davis and Ritchie (1986a) is used to scale up the model used for the humidity leach cell experiment. It was found from the modelling results and comparison with PYROX that the model under predicts the integrated sulphate production rate in the initial stages of the reacting waste heap dump. It does however show results that are in close agreement

with the results obtained from PYROX in later stages of the lifespan of the waste heap dump. This highlight limitations to the AAS model's applicability on geochemical problems. The model can only be applied to describe waste heap dumps where the particles at the top of the heap are fully oxidized.

Keywords: PHREEQC, Humidity leach cell, Pyrite, Kinetic modelling

List of Abbreviations

HLC	Humidity Leach Cell
ABA	Acid Base Accounting
PHEEEQC	A Computer Program for Speciation, Batch-Reaction, One-Dimensional Transport, and Inverse Geochemical Calculations
NAG	Net Acid Generation
ARD	Acid Rock Drainage
CSTR	Continuous Stirred Tank Reactor
SK	Surface Kinetic
ASTM	American Society for Testing and Materials
PYROX	Geochemical model developed by Wuderley and Blowes (1997)
ABATE	Acid-Base: Accounting, Techniques and Evaluation
1D	One Dimensional
2D	Two Dimensional
3D	Three Dimensional
XRD	X-Ray Diffraction
AAS	Approximate Analytical Solution
MATLAB	Mathematical program developed by MathWorks®
SCM	Shrinking Core Model
Ash Layer	Layer forming around the reactive core of a particle

Table of Contents

List of Figures

List of Tables

1. Introduction

1.1 Background

Several commercial geochemical models are available that has similar capabilities to that of PHREEQC (Parkhurst & Appelo, 2003), for example Geochemist's Workbench (Bethke, 1998) and POLYMIN (Molson *et al*., 2005). Geochemist Workbench has a friendly user interface and graphical output. The problem with commercial models are the associated cost which in certain cases restrict access to these software packages. It is shown in this dissertation that a reasonable model to describe HLC data can be developed using PHREEQC, which is an open source program available from the U.S. Geological Survey. It is further shown in literature that PHREEQC has the capabilities to model 1D reactive transport (Appelo & Postma, 2005). The use of PHREEQC to model column experiments is by no means novel; it is a general approach to model batch and flow reactors (Tiruta-barna, 2008).

Currently the ABATE strategy (Usher *et al*., 2002) or variations thereof is applied in South-Africa to develop a geochemical model to describe the impact of waste heap dumps or backfilling scenarios. Incorporating data obtained from these studies into a site specific geochemical numerical model is in most cases difficult. It is therefore important to model the data obtained from HCL tests and PHREEQC is used for this purpose. The following step is to up-scale the model results to represent field conditions to predict possible future seepage qualities that can be expected from these systems. It is shown from literature that the rate determining step governing the rate of pyrite oxidation can be attributed to diffusive oxygen transport into the heap (Davis, 1983). Modelling this behavior requires solving complex differential equations. Davis (1983) developed an analytical approximation to describe this behavior and can be implemented using PHREEQC.

1.2 Problem Statement

The majority of South African coal mines are opencast mines. The mining method results in back filled pits and above ground disposal facilities. Leachate emanating from these disposal sites is saline and could be highly acidic. Currently the standard testing procedure to quantify expected leachate qualities include Acid Base Accounting, Net-acid test, static-and kinetic leaching as outlined in the ABATE stategy (Usher *et al*., 2002).

It is required to incorporate data gathered from these tests in the development of a geochemical model that can be used to predict future water qualities expected from either waste heap dumps or back filled pits. The PHREEQC model will be applied to this problem.

1.3 Aims and Objectives

The aim of this dissertation is to investigate and develop methodologies to model geochemical problems applicable to waste heap dumps or discard dumps using PHREEQC (Parkhurst & Appelo, 2003). The objectives of the dissertation are listed below:

- Research and develop a methodology to model humidity leach cell behaviour using the PHREEQC code;
- Research methodologies that can be used to describe the physicochemical property governing leaching behaviour of waste heap dumps or discard dumps;
- Validate this methodology by comparing results obtained from this model to PYROX (Wunderley & Blowes, 1997);

The objectives listed above forms part of the strategy to develop a model in PHREEQC that utilises site specific data to model long term leaching behaviour of waste heap dumps.

2. Literature Survey

2.1 Introduction

Certain mining activities, including gold, nickel, copper and coal are known to promote the formation of acid mine drainage (AMD). AMD is commonly caused when sulfide-bearing materials are exposed to oxygen and water (Akcil & Koldas, 2006; Banwart & Malmström, 2001). Mining activities allows for oxygen to be introduced in deep geological environments containing minerals that are in a reduced state. The oxidation of iron disulfide (FeS_2), which is ubiquitous in most metal sulfides, is a complex series of reactions (Appelo & Postma, 2005). Section 2.2 includes a simplified set of reactions that is generally accepted to describe the formation of AMD.

2.2 Pyrite Oxidation

Pyrite oxidation is explained in this section by means of the following equations:

Equation 2.1

$$\mathrm{FeS_2} + {}^{7}/_{2}\,\mathrm{O_2} + \mathrm{H_2O} \rightarrow \mathrm{Fe^{2+}} + 2\mathrm{SO_4^{2-}} + 2\mathrm{H^+}$$

Equation 2.2

$$\mathrm{Fe^{2+}} + {}^{1}/_{4}\,\mathrm{O_2} + \mathrm{H^+} \rightarrow \mathrm{Fe^{3+}} + {}^{1}/_{2}\,\mathrm{H_2O}$$

Equation 2.3

$$Fe^{3+} + 3H_2O \rightarrow Fe(OH)_3 + 3H^+$$

Equation 2.4

$$FeS_2 + 14Fe^{3+} + 8H_2O \rightarrow 15Fe^{2+} + 2SO_4^{2-} + 16H^+$$

Younger (2000) suggests that a general reaction equation for the oxidation of pyrite can be written as Equation 2.5.

Equation 2.5

$$FeS_2 + \frac{15}{4}O_2 + \frac{7}{2}H_2O \rightarrow Fe(OH)_3 + 2SO_4^{2-} + 4H^+$$

In the first reaction, iron disulfide is oxidized, causing the formation of acid and the release of sulfate in the water. The ferrous iron (Fe^{2+}) can further be oxidized to Ferric iron (Fe^{3+}). The ferric iron can then either be hydrolyzed to form ferric hydroxide ($Fe(OH)_3$), also known as “yellow boy”, or the ferric iron can act as a catalyst in oxidation of iron disulfide (Skousen *et al.,* 2002). As discussed later in the literature, the main contributor to acidity in post mining water is metal sulfides. There are several reactions contributing to the buffering of a low pH resulting from the oxidation of pyrite. The most obvious of which is the dissolution of calcite ($CaCO_3$) (Bain *et al.*, 2001) and other carbonate rock forming minerals (dolomite and aragonite) (Appelo & Postma, 2005). The presence of buffering minerals affects the mobility of dissolved metals, for example the precipitation of gypsum may occur due to the increase of Ca^{2+} at the calcite dissolution front, thereby providing an upper limit on dissolved Ca^{2+} and SO_4^{2-} concentrations (Bain *et al.*, 2001)

It is well known from literature, (Appelo & Postma, 2005; Evangelou, 1995), that systems exposed to the atmosphere and those isolated from the atmosphere behave differently with regard to the dissolution and precipitation of carbonate minerals. In closed systems the sum of dissolved carbonates species are considered constant and the distribution of the dissolved species is a function of pH.

Equation 2.6 shows the relation of Ca^{2+} concentration and CO_2 pressure in the dissolution of $CaCO_3$ in pure water (Appelo & Postma, 2005).

Equation 2.6

$$m_{Ca^{2+}} = \sqrt[3]{10^{-6}\left[P_{CO_2}\right]/4}$$

where *m* refer to the to the concentration of Ca^{2+} and *P* denotes the partial pressure of carbon dioxide.

From previous research (Morin *et al.*, 1987) on areas affected by AMD it is shown that with the lowering of pH, secondary carbonates and hydroxide minerals may dissolve in a consistent sequence (Bain *et al.*, 2001).

With the initial flux of acid water, the first minerals to dissolve near the source are calcite, which will buffer the water close to a pH of 6. The following mineral is secondary siderite, buffering the pH near 5. After the depletion of siderite, gibbsite will start to dissolve, that results in a pH close to 4. Lastly any ferrihydrite will go into solution at a pH in the vicinity of 3. Buffering effects of minerals in the system is a critical control in the mobility of metals in AMD discharge (Banwart & Malmström, 2001). Silicate weathering also contributes to a buffering effect in post-mining water. This is a very slow process and the contribution will be a slow and gradual process (Appelo & Postma, 2005).

2.3 Reaction Kinetics

2.3.1 Surface reaction kinetics

Pyrite can either dissolve and then be oxidized or can be directly oxidized by either ferric iron or oxygen. The oxidation of pyrite by oxygen is shown in

Equation 2.1. The rate is generally reported to be very slow (Appelo & Postma, 2005).

Equation 2.4 shows the oxidation of pyrite by ferric iron. Reactions 1 and 4 depicted in Equation 2.1 and Equation 2.4 respectively, progress simultaneously as long as there is a reaction converting Fe^{2+} to Fe^{3+}.

Equation 2.2 shows the conversion of Fe^{2+} to Fe^{3+}. Based on Equations 2.1 and 2.4 the rate law for the oxidation of pyrite can be written as follows (Evangelou, 1995):

Equation 2.7

$$-\frac{d[FeS_2]}{dt} = [(k_1(O_2)^{v_1} + k_2(Fe^{3+})^{V_2}](S)$$

O_2 and Fe^{3+} refer to the partial pressure and concentration of O_2 and Fe^{3+} respectively. *S* is the surface area. The general rate law for the change in solute concentration due to the dissolution or precipitation of a mineral can be written as:

Equation 2.8

$$r_{mineral} = k\frac{A_0}{V}\left(\frac{m}{m_0}\right)^n g(C)$$

where $r_{mineral}$ denotes the overall reaction rate with the units [mol/l/s]. The constant *k* is the specific rate constant with the units [mol/m^2/s]. A_0 is the initial reaction surface area *V* is the reaction solution volume, m_0 the initial moles of solid mineral and *m* denotes the current moles of solid mineral in the system. The constant *n* is an empirical value relating to the change in reactive surface area. The function *g(C)* accounts for the effect of the solution composition on the rate equation. Typical examples are the pH of the solution or the distance from equilibrium. The factor $(m/m_0)^n$ accounts for the change in surface area where m_0 is the initial moles of the solid and *m* the moles at a given time (Appelo & Postma, 2005).

Kinetics reported by Williams and Rimstidt (1994) and also referenced by Appelo and Postma (2005) for the oxidation of pyrite by O_2 is documented as follows:

Equation 2.9

$$r_{pyrite_1} = 10^{-8.19} m_{O_2}^{0.5} m_{H^+}^{-0.11}$$

where $r_{pyrite1}$ is the overall pyrite reaction rate [mol/m^2/s]. It can be seen that the rate has a square root dependency on the concentration of O_2. This results in a significant effect on the rate for low oxygen concentrations and it has a small effect on the rate for high oxygen concentrations. This effect can be explained by the pyrite surface becoming saturated with O_2 (Appelo & Postma, 2005). The rate of pyrite oxidation by ferric iron is described in Equation 2.10 and the overall rate in Equation 2.11.

Equation 2.10

$$r_{pyrite_2} = 10^{-6.07} m_{Fe^{3+}}^{0.3} m_{Fe^{2+}}^{-0.32}$$

Equation 2.11

$$r_{pyrite_3} = 10^{-8.58} m_{Fe^{3+}}^{0.3} m_{Fe^{2+}}^{-0.47} m_{H^+}^{-0.32}$$

Fe^{2+} and H^+ compete with Fe^{3+} for sorption on the cathodic site of the pyrite, as can be seen by the negative affect the Fe^{2+} and H^+ concentration has on the rate law. The rates will increase infinitely with the decrease of Fe^{2+} and H^+ concentrations (Appelo & Postma, 2005). To avoid this infinite increase in a numerical model, an inhibitor factor is introduced that approach 1 when approaching a limiting concentration. The equation for the inhibitor factor is shown below:

Equation 2.12

$$(1 + \frac{m_{Fe^{2+}}}{m_{lim}})^n$$

The exponent *n* is an empirical coefficient and m_{lim} is a small limiting concentration. Using this inhibitor factor, Appelo and Postma (2005) propose the following rate equation for the oxidation of pyrite by oxygen and Fe^{3+}:

Equation 2.13

$$r_{pyrite_2} = 6.3 \times 10^{-4} m_{Fe^{3+}}^{0.92} (1 + m_{Fe^{2+}}/10^{-6})^{-0.43}$$

In the absence of oxygen Equation 2.13 is expressed as:

Equation 2.14

$$r_{pyrite_3} = 1.9 \times 10^{-6} m_{Fe^{3+}}^{0.28} (1 + \frac{m_{Fe^{2+}}}{10^{-6}})^{-0.52} m_{H^+}^{-0.3}$$

In many cases the equilibrium concept can give adequate explanation for what is observed in the system. This approach can however not account for the temporal nature of AMD. Appelo and Postma (2005) shows that the rate law for the oxidation of ferrous iron can be written as follows:

Equation 2.15

$$r_{pyrite_4} = -\frac{dm_{Fe^{2+}}}{dt} = k \cdot m_{Fe^{2+}} \cdot [OH^-]^2 \cdot P_{O_2}$$

The oxidation of pyrite at low pH is very slow, as can be inferred from the rate law by looking at the quadratic dependence of the OH^- concentration expressed in the rate law.

For the dissolution of a mineral depicted in Equation 2.16, Collon *et al.,* (2006) proposed a kinetic rate law for the modelling of geochemical reactions. This reaction is shown in in Equation 2.17:

Equation 2.16

$$A_n B \leftrightarrow nA^+ + B^n$$

In Equation 2.16, *A* and *B* denotes the reactant concentrations and *n* denotes the stoichiometric coefficient and the ion charge on the right hand side of the equation.

Equation 2.17

$$r(t) = \sigma k'_{pcp}[K(A_nB) - (A^+)^n(B^{n-})$$

In Equation 2.17, *r(t)* denotes the reaction rate, σ is a constant that is calculated in Equation 2.19, k'_{pcp} represent the reaction constant for precipitation and *K* is the equilibrium constant.

This rate law is based on an approach where two parameters are used to account for experimental results observed in closed reactor tests. With this approach the reaction rate is the difference between the rate of dissolution and the rate of precipitation, and can be written as:

Equation 2.18

$$r(t) = r_{diss} - r_{pcp}$$

To account for the variance in accessibility of minerals A_nB in natural rock and the induced variation of the apparent kinetic constants, K takes into account the relationship between the equilibrium and kinetic constant ($K = k'_{diss}/k'_{pcp}$). The specific surface is described by σ. This approach is similar to that expressed in Equation 2.8 (Appelo & Postma, 2005) and is presented in the equation below:

Equation 2.19

$$\sigma = F_g[m_{A_nB}(t)]^{2/3}$$

where *m* denotes the mass of the mineral. F_g expresses the influence of the specific surface of a rock volume on the reaction rate and can be calculated by the following equation:

Equation 2.20

$$F_g = 0.532\frac{6M_R}{G_R\rho_R}$$

In the equation above M_R represent the mass of rock per litre of water, G_R represent the mass fraction of the mineral in the rock and ρ_R denotes the density of the rock.

It is commonly observed that groundwater samples of completely flooded deep mines are much more polluted than when mining operations were still ongoing (Younger, 2000). The reason for this is the formation of 'acid-generating salts' according to Younger (2000). Pyrite oxidations start during mining operations in unsaturated areas in the mines. Due to the partially wetted conditions,

Equation 2.5 does not run to completion, causing the formation of intermediate solid phases. These intermediate products include the following minerals as shown in Table 2.1.

Table 2.1: List of possible acid-generating salts (Younger, 2000)

Mineral	Empirical formula
melanterite	$FeSO_4 \cdot 7H_2O$
römerite	$Fe^{2+}Fe^{3+}(SO_4) \cdot 14H_2O$
coquimbite	$Fe_2(SO_4)_3 \cdot 9H_2O$
copiapite	$Fe^{2+}Fe^{3+}(SO_4)_6(OH)_2 \cdot 20H_2O$
potassium jarosite	$KFe^{3+}(OH)_6(SO_4)_2$

2.3.2 Shrinking Core Model

A number of mathematical models to describe the kinetics of a heterogeneous reaction have been developed over the years. These models were developed for describing leaching behavior of copper heaps. Davis and Ritchie (1985a) refer to three primary types that all describe in-situ leaching behavior by focusing on the leaching behavior of the individual particles in the heap (Figure 2.1). All three these modelling approaches assume the particle is spherical and that the reaction front moves radially towards the center of the particle (Davis & Ritchie, 1985a; Mayer *et al*., 2002).

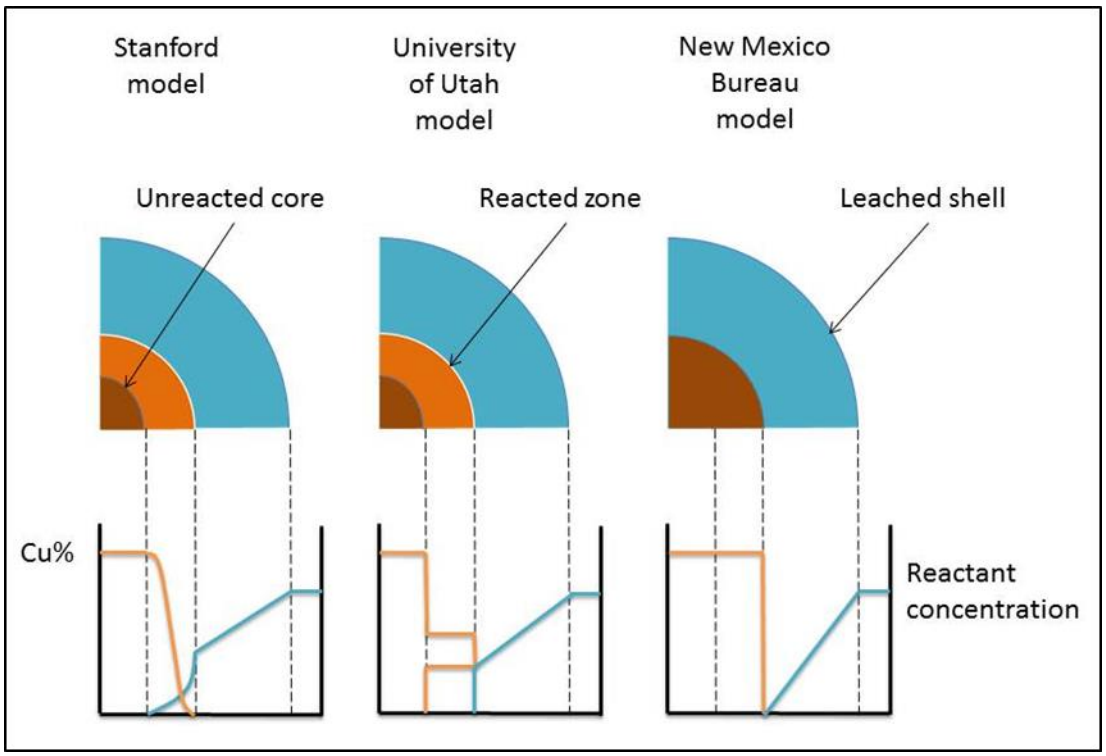

Figure 2.1: Schematically drawing of the three leach models discussed by Davis and Ritchie, (1986a)

According to Davis and Ritchie (1986a), the three models differ in the assumptions made about the reaction rate compared to the reactant transport rate of the reaction sites.

The most well-known and widely used of these models is the Shrinking core model (SCM). This mathematical model describes the kinetics for a solid-gas and solid-liquid system (Levenspiel, 1999). The model finds it application in geochemistry by describing the oxidation of pyrite in heap leaching scenarios. For a heterogeneous reaction in which a fluid reacts with a solid the following reaction applies:

Equation 2.21

$$A(fluid) + bB(solid) \rightarrow solid\ products + fluid\ product$$

In the equation above the parameter *b* represent the stoichiometric coefficient of reactant *B*. The rate of reaction can be controlled by three mechanisms, the first of which is diffusion through the gas film. This is not discussed further in this dissertation, as it is assumed that the reaction of the particles occur at the water-solid

interface (Mayer *et al.*, 2002). The second rate determining step is the diffusion of the reactant through the ash layer and can be mathematically described as follows:

Equation 2.22

$$-\frac{\mathrm{dN_A}}{\mathrm{dt}} = \mathrm{r_{mineral}} = 4\pi \mathrm{r}^2 \mathrm{D}_2 \frac{\mathrm{dC_A}}{\mathrm{dr}}$$

where *r* is the radius of the unreacted core [m] and D_2 is the diffusion coefficient of the reactant through the ash layer [m^2/s]. The ash layer or alteration rim refers to the reacted crust that forms around the unreacted core (Figure 2.1). The third rate determining step is chemical rate controls, and can be mathematically expressed as follows:

Equation 2.23

$$-\frac{1}{4\pi r^2}\frac{dN_B}{dt} = r_{Mineral} = \frac{-b}{4\pi r^2}\frac{dN_A}{dt} = bk'' C_{Ag}$$

where *k''* is the first order rate constant for the surface reaction and C_{Ag} is the gas phase concentration of the reactant diffusing through the ash layer [moles/l]. Mayer *et al*. (2002) only distinguish between transport-controlled and surface-controlled reactions. Levenspiel (1999) shows that the abovementioned rate controlling steps can be combined to account for the influence of all three rate controlling steps:

Equation 2.24

$$-\frac{dr}{dt} = r_{Mineral} = \frac{{bC_A}/{\rho_B}}{\frac{(R-r)r}{RD_2} + \frac{1}{k''}}$$

where *R* is the radius of the initial unreacted particle and the density of the particle is denoted by ρ_B [kg/m^3]. Ardejani *et al*. (2008) used this approach to describe the kinetic oxidation of pyrite.

2.4 Predictive Methods

In order to implement a successful environmental strategy, the source of pollution risk must be identified and there must be a good understanding of how this risk might evolve at the site in question (Berger *et al.*, 2000; Linklater *et al.*, 2005). According to Nordstrom (2010), several points must be raised when looking at geochemical modelling. Firstly when referring to a model, it does not necessary imply that the model is a computer code or a mathematical approach. It can consist of a well constrained logical proposition with the goal to improve or refine a conceptual model of the problem. Usher *et al.* (2002) proposed the ABATE strategy as an all-inclusive approach of methodologies to develop a geochemical model as shown in Figure 2.2. A geochemical model can provide invaluable insight with regards to understanding environmental risk and can assist in the interpretation of field data (Linklater *et al.*, 2005).

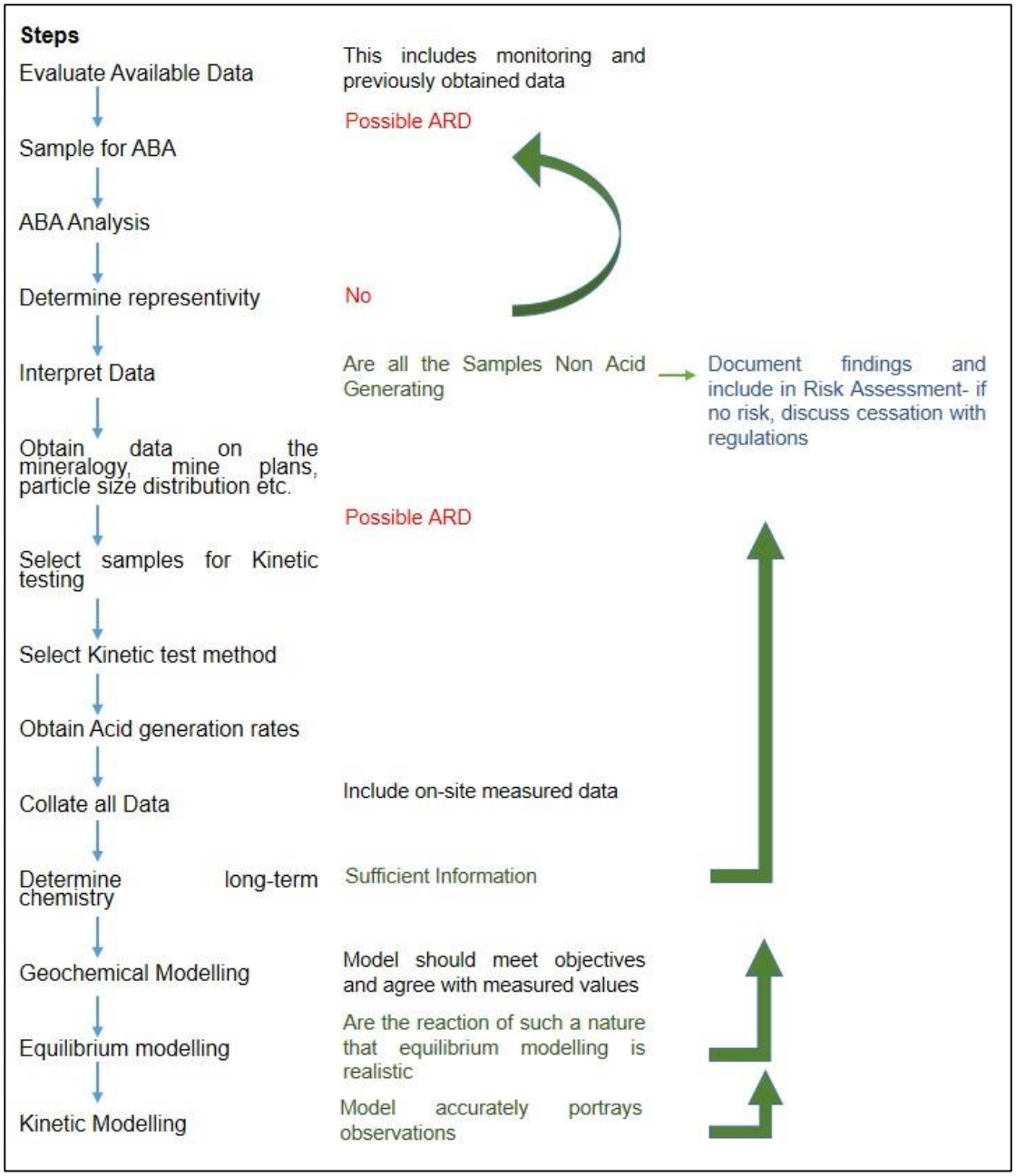

Figure 2.2: Flow diagram of the ABATE strategy (Usher *et al.*, 2002)

2.4.1 Static test

ABA is generally used as a first order classification procedure in acid rock drainage (ARD) prediction methodologies. ABA results provide information about the potential of a sample to generate ARD (Price, 1997); it is a valuable and widely used test that determines both the acid-generating and acid neutralizing potential of a sample (Skousen *et al.*, 2002). Net Acid Generating (NAG) tests are also performed to aid in a better interpretation of the ABA results (Miller *et al*., 1997). The test procedure is not time consuming, is low cost and the analytical procedure is relatively simple (Usher *et al*., 2002).

There is however limitations to this test procedure. The most important of which is the fact that ABA does not address the transient behavior of ARD and this is also the case for all the static type tests. Usher *et al.* (2002) notes that the ABA test procedure assumes instant availability of reactants, simple reaction stoichiometry and account for size effects of solid reactants.

2.4.2 Kinetic tests

In order to address the shortfalls of static testing Usher *et al*. (2002) recommends a kinetic leach test methodology adapted from the D5744-96 Standard Test Method (ASTM, 2001). The minimum suggested duration of this leach test is twenty weeks and is in some cases not enough time for sulphate production to stabilize. Humidity cell tests (HCT) supplement static tests in this regard, and can assist in obtaining reaction rates and an indication of the potential mineral leaching behavior of rock samples (Price, 1997). Currently one of the biggest challenges faced by environmental practitioners is to integrate site specific data obtained from HCT's into predictive geochemical models (Sunkavalli, 2014).

2.5 Modelling of acid mine drainage

Mathematical models have become an integral part of the development of a geochemical model and are the last step in the ABATE strategy. Modelling the evolution of water chemistry as it leaches through a waste heap dump can become very complex, as there are multiple processes influencing the change in leachate composition. Geochemical reactions that may occur include aqueous speciation, precipitation and dissolution of minerals, ion exchange and redox reaction (Wunderley *et al*., 1995; Linklater *et al*., 2005)

Both equilibrium and reaction path geochemical models can be used to describe the formation of AMD. They can be linked with a combination of different transport models for CSTR, 1D, 2D, 3D transport and dynamic or steady state conditions (Andre, 2009). It is seen from literature that a purely equilibrium based model is not sufficient to describe AMD (Appelo & Postma, 2005; Andre, 2009). This is due to the slow reaction kinetics of pyrite oxidation. Wunderley *et al.* (1995) states that when reactions between solid minerals and reactants in the aqueous phase are rapid it is valid to adopt an equilibrium mass-action approach to the geochemical model. For this assumption to be valid, the rate of reaction between the solid minerals and the aqueous phase must be infinitely faster than the governing flow phase (Brown *et al.*, 1999). For a heap leach scenario this assumption is not valid, reactions are

described kinetically. In these systems there are several rate determining factors. The general approach to the modelling of AMD is assuming that oxygen diffusion is the rate determining step in the oxidation of pyrite. In the well-known work done by Davis and Ritchie (1986a) and later also by Molson *et al*. (2005), the shrinking core model is used to describe the reaction kinetics of pyrite oxidation in a waste heap. In this approach it is assumed that the rate of oxygen diffusion of the reaction sites is the rate limiting step. This is also discussed as an important factor in the oxidation of pyrite soils by Appelo and Postma (2005). It is noted that oxygen transport is only important in the unsaturated zone. In the saturated zone, the approximate amount of oxygen available for pyrite oxidation is 0.33 mM O_2, suggesting that the unsaturated zone is the most reactive and the greatest source of sulphate oxidation.

Davis and Ritchie (1985a) further assume that the rate of unreacted core shrinkage is much slower than the oxygen diffusion rate within the particle. It is further assumed that the reaction at the surface of the particle is instantaneous and that the ash layer diffusion is the rate determining step.

In the model developed by Davis and Ritchie (1986a) it is assumed that diffusion is the only means of oxygen transport. Fick's second law (Equation 2.25) with a consumption term is used to describe the diffusion process mathematically:

Equation 2.25

$$\frac{\partial U_A}{\partial t} = D_1 \frac{\partial^2 U_A}{\partial z^2} - q(z,t)$$

The model describes a two-stage diffusion process to the reaction sites. The first stage consists of oxygen diffusion through the air filled pores. D_1 is the diffusion coefficient for this stage. The consumption term $q(z,t)$ represents the change in volume due to the oxidation of pyrite, and can be expressed as Equation 2.26 (Molson *et al*., 2005).

Equation 2.26

$$q(z,t) = D_2 \frac{3(1-\theta)}{R^2} \left(\frac{r}{R-r}\right) \frac{[O_2]_a}{H}$$

where H is Henry's constant [kg/m^3] and $[O_2]_a$ is the concentration of oxygen in the pore space. D_2 represents the diffusion coefficient for the forming ash layer shielding the shrinking particle. The concentration of oxygen dissolving into the water film surrounding the particle is calculated using Henry's law, where H represents Henry's constant for a given temperature. The parameter θ represents the gas filled porosity of the material. Figure 2.3 show a schematic drawing of the shrinking core model.

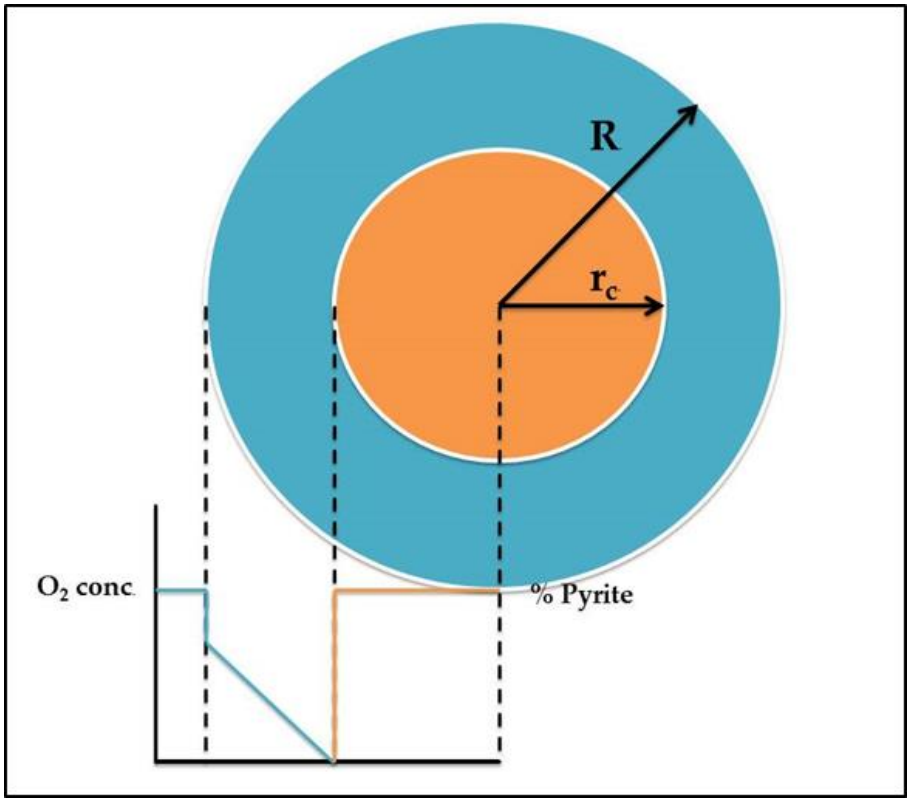

Figure 2.3: Schematic representation of an oxidizing particle (Davis, 1983)

It can be seen from Figure 2.3 that a ash layer forms around the reacting particle core. Oxygen diffuses from surface of the particle through the ash layer to the unreacted core.

From Equation 2.26 and Figure 2.3 it can be seen that the change in oxygen due to pyrite oxidation can be related to the change in the unreacted core radius (r):

Equation 2.27

$$\frac{dr_c}{dt} = \frac{D_2(1-\theta)}{\epsilon\rho_s}\frac{R}{r(R-r)}\frac{[O_2]_a}{H}$$

where ε is the ratio of oxygen to sulphur consumed on the basis of the reaction stoichiometry and r_c represents the reaction rate. R represents the initial unreacted core radius and r is the transient unreacted core radius. The density ρ_S is calculated from the bulk density and the weight fraction of pyrite present.

The majority of the most recent geochemical models used to model the oxidation of pyrite in waste heap dumps are based on the approach outlined above (Linklater *et al.*, 2005; Gerke *et al.*, 2001; Molson *et al.*, 2008; Bain *et al.*, 2001; Brown *et al.*, 1999).

2.6 Modelling spoils heaps

Substantial work has been done on the importance of chemical, physical and microbiological factors influencing the weathering rate of pyrite (Linklater *et al.*, 2005, Molson *et al.*, 2008).

Leaching of metals contained in the constituents of mining ore or the leached product or spoils heaps and tailings dams rely on the oxidation of insoluble sulphide bearing minerals to soluble sulphates (Davis & Ritchie, 1986a). Water transports the soluble oxidation products through the gangue where further oxidation, dissolution and precipitation can take place (Brown *et al.*, 1999). Thus the concentration of chemical constituents in the effluent of a spoils heap is space and time dependent, which in turn depend on the pyrite oxidation rate, water infiltration rate and the chemical oxidation rates (Pantelis *et al.*, 2001).

Several mathematical models describing the leaching process in spoils heaps, have been developed over the last couple of years (Davies & Ritchie, 1986; Molson *et al.*, 2005; Linklater *et al.*, 2005; Pantelis *et al.*, 2001). In the work done by Davies and Ritchie (1986a) it is assumed that oxygen is transported into the heap by means of diffusion. In the work conducted by Lefebvre *et al.*, (2001) it is shown that the convective flow of oxygen caused by heat production of pyrite oxidation can also determine the rate of oxygen supply. Pantelis *et al.* (2001) modelled the spoils heap as a three-phase system consisting of gas and water phases flowing through a rigid solid porous phase. To simplify the mode it was assumed that the sulphide containing minerals consist entirely of pyrite. There was also no compensation for the temperature dependence of the diffusion coefficients, viscosities and thermal conductivities. This was done under the assumption that physical conditions in the spoils heap reach pseudo steady state which can last in most cases for decades or longer.

The pH of the spoils heap effluent is controlled by several factors. Strömber and Banwart (1999) identified two main controls, namely sulphide oxidation with calcite dissolution that can sustain a neutral pH and simultaneous oxidation of sulphide and weathering of primary silicates. The latter is characterised by effluent water with a pH between 3 and 4.

3. Development methodology and model code

3.1 Introduction

In the previous chapter the approach to developing a geochemical model was discussed. It was noted that there are challenges to integrate site specific data obtained from HCT into a geochemical model. In this chapter the development of a model will be discussed to address this problem. The model is based on surface kinetics (Surface Kinetic Model). This model will be used to simulate a standard humidity cell leach test (ASTM, 2001). The next step is to scale the model up to field conditions by making use of the of the Approximate Analytical Solution or AAS method as developed by Davis and Ritchie (1986a). The model will be simulated using PHREEQC (Parkhurst & Appello, 2003), and compared to results obtained from PYROX (Wunderley & Blowes, 1997). The mathematical governing equations are discussed and the derivations shown which are used to describe the geochemical system.

3.2 Modelling HCT with the Surface Kinetic Model

Several rates that describe the oxidation of pyrite and the factors that influence the rate of reaction were discussed in the previous chapter. Following the steps set out in the ABATE strategy; the next step, following data collection, is the development of a geochemical model. Site specific data were obtained by means of a HCT. The HCT data were modelled using PHREEQC code. PHREEQC has the ability to model dynamic processes such as reaction kinetics, 1D reactive transport through the use of the RATES block and TRANSPORT block respectively.

Simulating this process using PHRREEQC is complex and several approximations are required. The basic physiochemical parameters governing the system will be discussed first to define the system.

Air is introduced into the system by pumping ‘dry air’ into the cell; this is followed by air that has been passed through a humidifier. This usually consists of a three day period for each air cycle. The two air cycles are then followed by leaching the cell with deionized water. Figure 3.1 shows a simplified schematic drawing of the system in question.

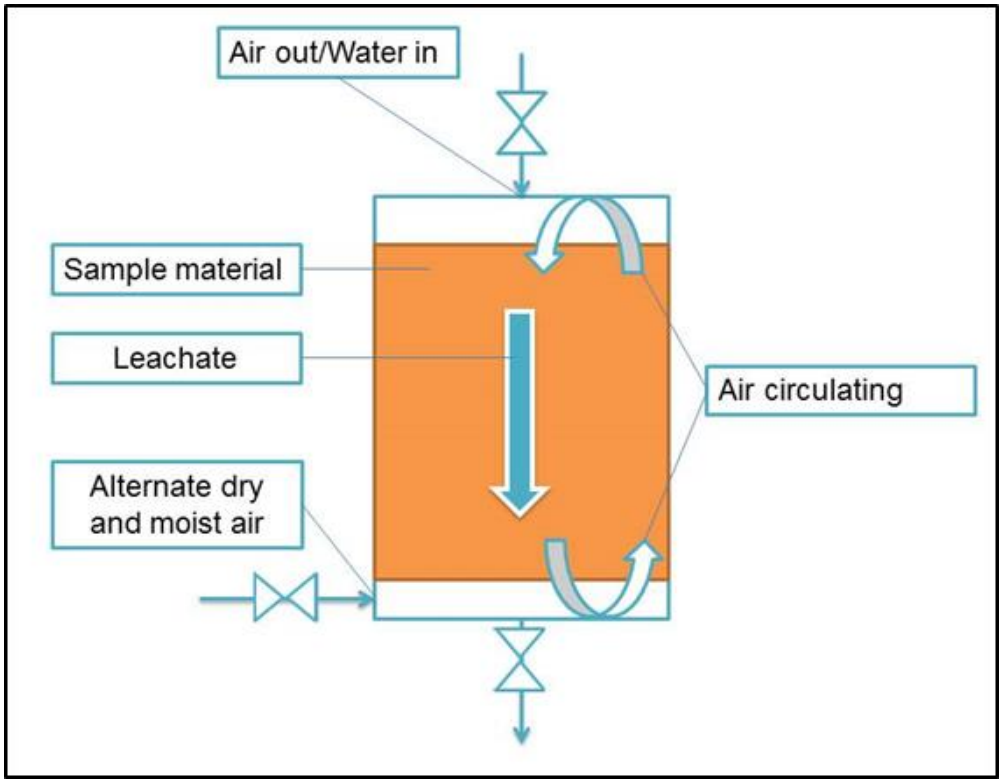

Figure 3.1: Basic schematically drawing of a HCT after Usher *et al*. (2002)

The objective of circulating dry and moist air through the system is to accelerate the weathering rate of the sample. The final leach step is then used to remove the weathered products from the system.

In order to describe the behavior of a HCT by making use of geochemical modelling, several assumptions are required to sufficiently simplify the system. The following main assumptions that were applied are as follows:

- oxygen is assumed to be in excess;
- there are no stagnant zones in the leach column and all the particles are exposed to the deionized water for the same period of time; and
- the residence time of the leachate in the cell is equivalent to one leach cycle.

The assumptions listed above allow the HCT to be approximated as a continuous stirred tank reactor (CSTR). Equation 3.1 describes the residence time of the leachate within the cell or reactor:

Equation 3.1

$$\tau = V_{tank}/(dV\ /\ dt)$$

The parameter τ represents residence time and V_{tank} the leachate volume of the system.

Figure 3.2 depicts the CSTR approach to modelling a HCT. The leachate movement through the particles comprising the sample is described as a well-mixed reactor. It is assumed that all the particles in the cell come into contact with the leachate in the form of a thin liquid film forming around the particles. The assumption that oxygen is available in excess is valid as air is pumped into the cell and is circulated through the sample material. It is further assumed that the liquid film surrounding the particle is thin, and is negligible compared to the area of the particle exposed to air, which leads to the assumption that there is no rate limiting effects in terms of oxygen transport to the reactive zone.

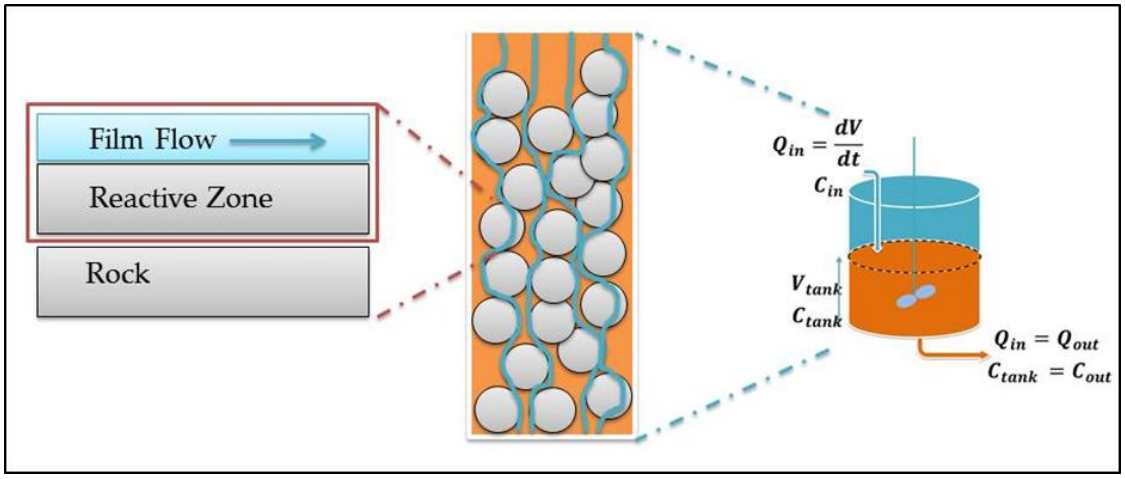

Figure 3.2: Basic schematically drawing of a HCT after Andre (2009)

The concentration of O_2 in solution can then be calculated using Henry's law. Usually the Henry's law constants are reported at a reference temperature of 25°C and 1 atm. The temperature can be evaluated through the use of Equation 3.2 and Equation 3.3 (Koretsky, 2003):

Equation 3.2

$$\left(\frac{\partial lnH_i}{\partial P}\right) = \frac{H_i^{\infty} - h_i^{v}}{R}$$

Where R is the gas constant, H_i^{∞} are the partial molar enthalpy and h_i^{v} the pure species enthalpy. A similar equation describes the correction for pressure, but it is beyond the scope of this dissertation as the pressure will always be assumed to be at 1 atm. Assuming the mole fraction of oxygen in ambient conditions is 0.21, the partial pressure of O_2 is then calculated using the following equation:

Equation 3.3

$$P_{O2} = (0.21)P$$

The concentration of oxygen in solution is calculated through the use of Henry's coefficient for oxygen in water ($\mathrm{H}_{O2} = 44252.9\ Bar\ @\ 25℃\ and\ 1\ atm$), and is expressed in the following equation:

Equation 3.4

$$x_{O2} = \frac{y_{O2}P}{H_{O2}} = \frac{0.21[bar]}{44253.9[bar]} = 4.75 \times 10^{-6}$$

The concentration of oxygen [O_2] in molality is expressed as follows:

Equation 3.5

$$[O_2] = \frac{n_{O2}}{V}$$

where *V* is 1 liter of water and n_{O2} is the molar amount of O_2 dissolved. The concentration of dissolved oxygen can then be calculated through Equation 3.6.

Equation 3.6

$$[O_2] = x_{O2}\frac{n_{O2}}{V} = 2.63 \times 10^{-4}[M]$$

This can be simulated in PHREEQC by making use of the EQUILIBRIUM_PHASES block. The liquid is equilibrated with air at a defined temperature. Figure 3.3 shows an example of PHREEQC code that calculates the molar amount of oxygen that dissolves in water at 25°Celcius. The amount of oxygen is expressed as the log value of the partial pressure of oxygen, in this case 0.21 atm.

```
SOLUTION 1
temperature 25
EQUILIBRIUM_PHASES
O2(g)          -0.677780705
END
```

Figure 3.3: PHREEQC code that calculated the molar amount of dissolved oxygen

3.2.1 Developing a methodology to describe a CSTR in PHREEQC

Following the methodology described by Tiruta-Barna (2008), a mass balance is conduct over a finite element as shown in Figure 3.4.

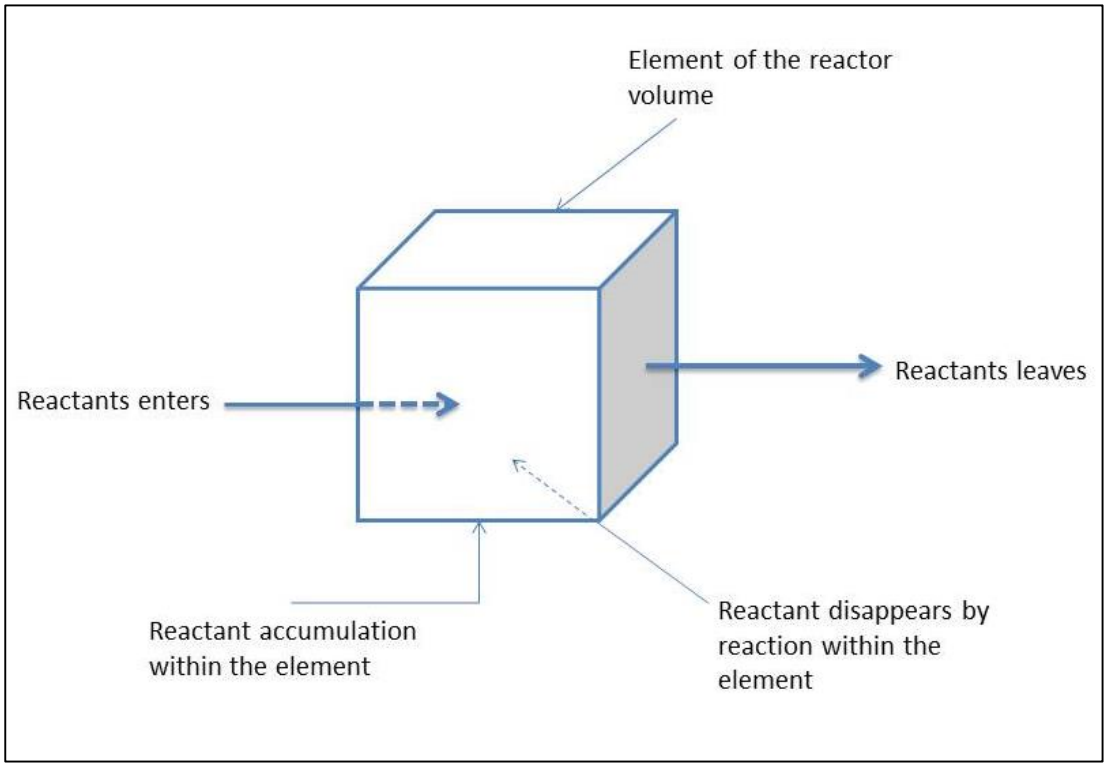

Figure 3.4: Material balance for an element of volume of the reactor (Levenspiel, p84)

The mass balance depicted in Figure 3.4 is achieved through the following equation:

Equation 3.7

$$\left(\frac{dc'}{dt}\right) = \left[\frac{Q}{V_{leachate}}(c'_{in} - c')\right]_1 + [\sum v_k R_k]_2$$

where ***c'*** denotes the concentration of the reactant c, $V_{leachate}$ refer to the volume of solute in the system.

The term numbered with subscript 1 is the convection term and the term 2 is the reaction kinetics. The CSTR equation is modelled in PHREEQC by solving the differential equation in the RATES block. This is accomplished through the use of PHREEQC`s Runge-Kutta integrator. A fragment of the code is depicted in Figure 3.5 to solve the following differential equation (Tiruta-Barna, 2008):

Equation 3.8

$$\frac{dc'}{dt} = \frac{Q}{V_{leachate}}(c'_{in} - c')$$

The analytical solution to Equation 3.8 is given as:

Equation 3.9

$$c' = c'_0 exp\left(-\frac{tQ}{V_{leachate}}\right)$$

where ***c'*** is the current concentration of reactant in the reactor, *Q* is the volumetric inflow rate of liquid into and out of the reactor and $V_{leachate}$ is the volume of the reactor.

The solution obtained from PHREEQC is compared to the analytical solution in Figure 3.5.

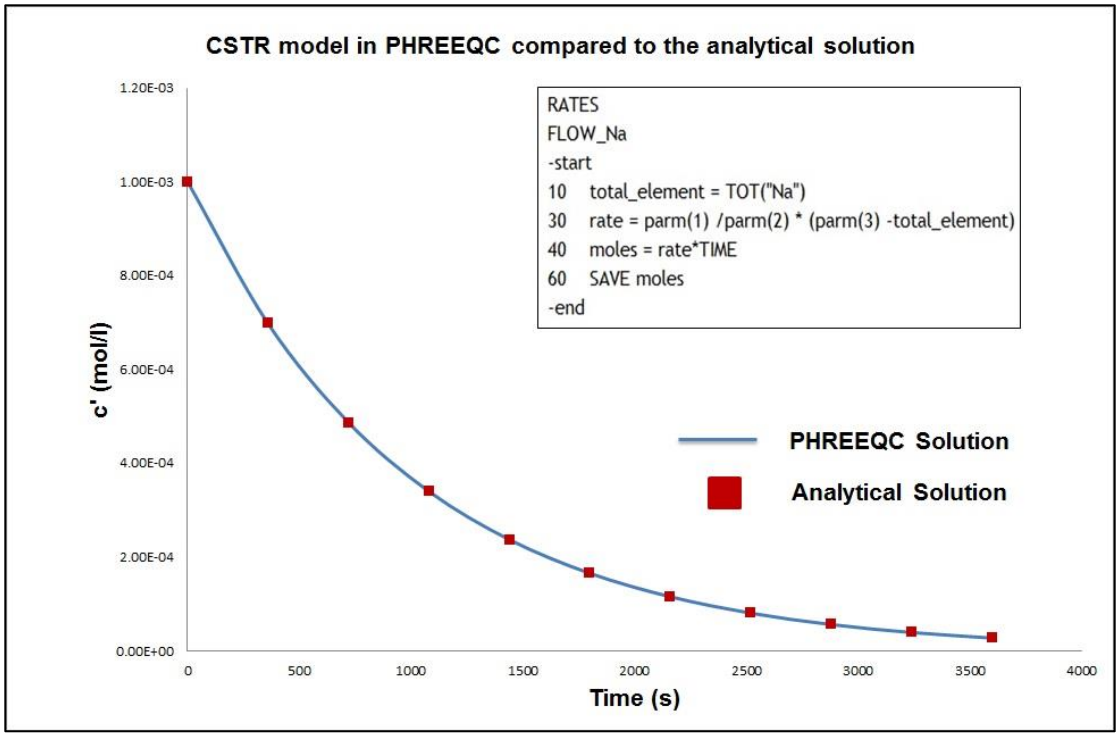

Figure 3.5: Fragment of a PHREEQC code used to model a CSTR by making use of the RATES block (Tiruta-Barna, 2008)

Now that a solution for the convection term of the CSTR exists, the reaction kinetic term of

Equation 3.7 needs to be addressed. It is proposed to model the convection term using the TRANSPORT block in PHREEQC and model the reaction kinetics using the RATE block. The TRANSPORT block has the capability to call up the calculations of the RATE block to simulate the rate kinetics. The TRANSPORT block also has the capability to simulate multicomponent diffusion in an aqueous solution. All chemical processes in PHREEQC can be included in the transport simulation (Parkhurst & Appelo, 2003). In the work conducted by Appelo *et al.* (1997) this methodology is used to model the evolution of leachate through a column containing pyrite and marine sediment. Nicholson *et al*. (2003) also used the 1D transport capabilities to model waste rock piles containing uranium for closure purposes. In the abovementioned studies the column is modelled by dividing the column into a number of nodes. Figure 3.6 depicts a conceptual drawing of the modelling approach used in PHREEQC to model 1D reactive transport.

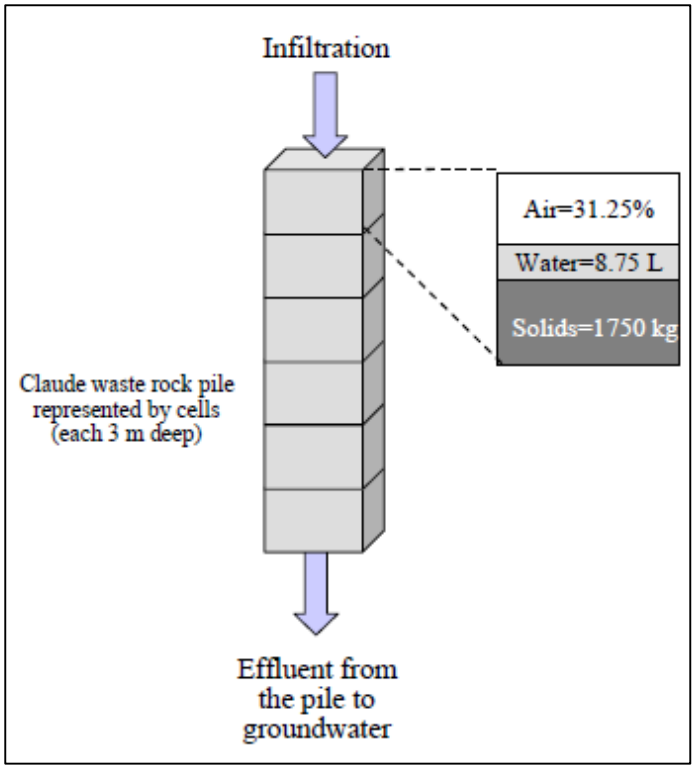

Figure 3.6: Conceptual model of a column modelled in PHREEQC by making use of the 1D transport capabilities of the software (Nicholson *et al*., 2003)

Stagnant cells can be added to the 'active cells' to model stagnant zone or radial diffusion. This functionality can be used to implement a CSTR. In the TRANSPORT block stagnant cells can be defined that can be used to interact with 'active' transport cells using the MIX block to model the Q value defined in Equation 3.7. Reaction kinetics and solution composition can then be defined for individual 'active cells' or nodes. Boundary conditions can also be implemented (Parkhurst & Appelo, 2003). The first is the Dirichlet boundary condition where the concentration is constant and known:

Equation 3.10

$$C(x_{end}, t) = C_0$$

The second boundary condition is the no flux boundary condition or Neumann boundary condition:

Equation 3.11

$$\frac{dC(x_{end},t)}{dx} = 0$$

The third boundary condition is known as the Cauchy boundary condition or flux boundary condition:

Equation 3.12

$$C(x_{end},t) = C_0 + \frac{D_L}{v}\frac{dC(x_{end},t)}{dx}$$

where D_L is the dispersion coefficient [m^2/s]. The Dirichlet- and Cauchy boundary conditions are then used in an 'active cell' to mix with a stagnant cell where the flow direction defined in the TRANSPORT block is diffusion only. The flow rate into and out of the reactor (the 'active cell') can then be set by the shifts input. The shifts input define the rate at which the leachate moves through each cell. This methodology was adopted from a similar approach developed by Tiruta-Barna*et al.* (2006).

3.3 Model setup in PHREEQC

3.3.1 Defining the reaction kinetics

Following the methodology proposed by Appelo and Postma (2005) the reaction rate for the dissolution/precipitation can be modeled by combining Equation 2.8 and Equation 2.9 resulting in the following equation:

Equation 3.13

$$R = A_0\left(\frac{m}{m_0}\right)^n (10^{-8.19} m_{O2}^{0.5} m_{H+}^{-0.11})(1 - IAP/K)$$

The ion activity product, IAP, has an influence on the rate of reaction and has an important influence on the rate as the solution approach equilibrium. For the dissolution of gypsum the same methodology was followed, rendering the following rate law for the dissolution of gypsum

Equation 3.14

$$\frac{d[Ca]}{dt} = 3.1 \cdot 10^{-8} A_0 (1 - IAP/K)$$

The kinetic dissolution of dolomite can be described by the following rate equation (Appelo & Postma, 2005):

Equation 3.15

$$r = \frac{dCa}{dt} = -k_d \cdot \ln(\frac{AI}{K_{dol}})$$

This is a very elementary rate equation and several more complex rate equations were developed that describe the dissolution of dolomite under different condition (Brown*et al.*, 2003; Zhang *et al*., 2007; Pokrovsky*et al*., 2009). Partial pressure of carbon dioxide, temperature and concentration of magnesium can influence the dissolution rate of dolomite. Several kinetic rate laws are defined in the default PHREEQC database. These rates can be used in the simulations through the KINETICS block.

3.3.2 Equilibrium phases

Several minerals dissolve or precipitate fast relative to the oxidation of pyrite or the dissolution of silicate minerals. The reactions of these minerals can then be described as equilibrium controlled as they happen instantaneous compared to the time scale of minerals like pyrite to react. Common equilibrium reactions found in waste heaps that is likely to occur, is the dissolution and precipitation of gypsum (Nicholson *et al*., 2003). In PHREEQC the EQUILIBRIUM_PHASES block is used to define these minerals. It is assumed that these reactions occur instantaneous and is controlled by the solute composition and can be described by the law of mass action:

Equation 3.16

$$aA + bB \leftrightarrow cC + dD$$

Equation 3.17

$$K = \frac{[C]^c[D]^d}{[A]^a[B]^b}$$

Secondary minerals that may precipitate are also defined in the EQUILIBRIUM_PHASES block.

3.3.3 Calculating composition from mineralogy

The composition of the HLC column is determined by making use of the mineralogy data obtained from the XRD analysis that can be found in Appendix A. A mass of 1000 grams was used in the HLC. The XRD data provides a mass percentage for the minerals present in the sample. From this the molar amounts of each mineral present can be calculated as shown in Table 3.1.

Table 3.1: Calculated molar amounts of HLC

Composition		
Mineral	Amount	
	(weight %)	moles
Anatase	5.45	0.682
Calcite	6.22	0.621
Dolomite	15.17	0.823
Kaolinite	61.6	2.386
Pyrite	5.43	0.453
Quartz	6.13	1.020

It is assumed that quartz will not react in the HLC as the reaction of this mineral is very slow relative to the duration of the test and therefore is not considered in the model.

3.3.4 Defining the reaction surface

The reactive surface area of the minerals in the HLC is unknown and will be used as a fitting parameter. The reaction surface can be approximated using the following equation:

Equation 3.18

$$S = \left(\frac{6}{d}\right)\lambda$$

where *d* is the diameter of a spherical particle and λ is surface roughness factor. The latter is defined as the ratio of the true reactive surface area to the equivalent geometric surface area.

3.4 Up-Scaling to Field conditions

The second problem that needs to be addressed in is the integration of data obtained from static and kinetic tests into a geochemical model that describe field conditions. For this purpose, methods for modelling physical and chemical processes described in literature must be implemented in PHREEQC. The discussion below describes the conceptualisation and development of theory that are widely used today in geochemical models to describe waste heap dumps (Pantelis *et al.*, 2001).

Ritchie (1977) developed a mathematical model to better understand the rate limiting mechanisms of pyrite oxidation in waste heap dumps. The model also aimed to address the various parameters governing the active transport behavior in the heap. The model considered the heap to be a homogeneous semi-infinite slab (Davies, 1983). It was assumed that oxygen transport to the reaction sites in the heap was the main rate determining mechanism. All reactants besides oxygen were assumed to be available, including bacteria catalyzing the oxidation reaction of pyrite. It was seen that the catalyzing effects of bacteria had little effects on the model as the rate of reaction was already assumed to be controlled by the availability oxygen in the heap. For this reason Davis and Ritchie (1986a) adopted the planar moving boundary approach to model the reactions in the waste heap dump.

It was assumed that the diffusion of oxygen through pore space of the heap was the rate controlling step and therefore it implied that the oxygen arriving at the reaction sites reacted instantly with the pyrite, resulting in a zero oxygen concentration at this point. The mass flux of oxygen through the reaction boundary in the model developed by Ritchie (1997) was assumed to be the velocity of the moving front, depending explicitly on the density of pyrite in waste dump, the ratio of oxygen consumed to pyrite reacted in the oxidation reaction and the diffusion coefficient of oxygen within the pores pace of the dump (Davies, 1983).

Davies (1983) extended this model by implementing a two stage model. The first stage is the diffusional transport of oxygen from the atmosphere, through the pore space, to the particles in the heap. The second stage describes the transport of oxygen to the reaction sites through the ash layer. The model proposed by Davies (1983) and later published in as a series of three very insightful articles (Davis & Ritchie, 1986a, b, c) will be followed in an attempt to model waste heap dumps and the backfilled pits by incorporating data obtained from static and kinetic tests as outlined in the ABATE strategy described in Chapter 2.

3.4.1 Oxygen transport

In Chapter 2 the mass balance in the pore space of a dump governed by diffusive transport was discussed. In order to use this equation, it must be assumed that all the particles are spherical and identical in size. The mass balance for oxygen in the spherical particle is given by the following equation (Molson *et al.*, 2005):

Equation 3.19

$$\frac{dr}{dt} = D_2 \frac{3(1-\theta_s)}{R^2}\left(\frac{r}{R-r}\right)\frac{[O_2]_a}{H}$$

where D_2 is the effective diffusion coefficient, incorporating the diffusion properties of oxygen in water through the ash layer. The last term in the equation denotes the concentration of oxygen in pore space, where *H* represent Henry's coefficient. This term calculates the molar concentration of oxygen in the liquid film surrounding the particle. R represents the particle's unreacted radius at time t = t_0.

3.4.2 The Approximate Analytical solution

The conceptual model of a waste heap dump is shown in Figure 3.7.

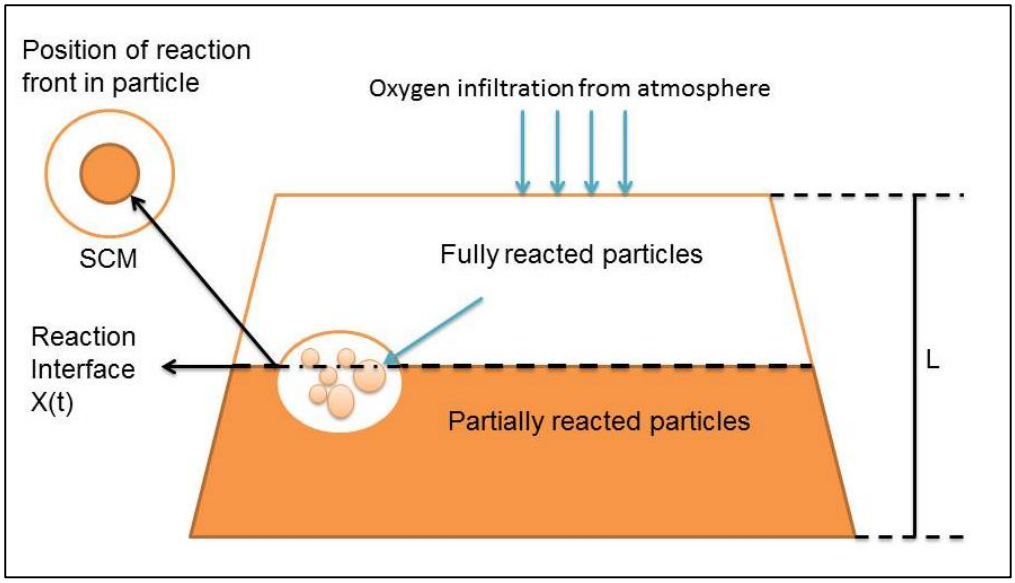

Figure 3.7: Conceptual diagram of a waste heap dump depicting the basic approach by Davis and Ritchie (1986a)

In order to model the waste heap dump as described by Davis and Ritchie (1986a) a pseudo-steady state approximation for the particles in the dump is assumed, rendering a set of two equations:

Equation 3.20

$$\delta_1 \frac{du}{dt} = \frac{d^2u}{dx^2} - 3k\frac{uR}{[1-R]} \; for \; 0 < x < 1$$

Equation 3.21

$$\frac{dR}{dt} = -\frac{ku}{R(1-R)} for \; 0 < R < 1$$

The symbol *u* represent the oxygen concentration, *R* the position of reaction front within the particle [m]. The following boundary and initial conditions apply to the above equations:

$$u(0,t) = 1$$

$$\frac{du}{dx} = (1, t) = 0$$

$$u(x, 0) = 0$$

$$R(x, 0) = 1$$

This set of equations needs to be solved numerically. Davies and Ritchie, (1986a) proposed an analytical solution to this system. The following analytical equations form part of the solution to the above set of differential equations:

Equation 3.22

$$t_c = \frac{1}{6k}$$

This equation is used to calculate the time it takes for the reaction front *X(t)* to reach the top of the waste heap dump, i.e. the time it takes for the particles on the surface of the heap to be fully oxidized as described by the shrinking core model. The constant k is calculated as follows:

Equation 3.23

$$k = \frac{k_1}{3}$$

The constant k_1 is calculated by the following equation:

Equation 3.24

$$k_1 = \frac{3\gamma D_2(1-\rho)L^2}{(D_1 a^2)}$$

where the γ denotes a proportionality constant that include both the Henry's law and gas law. The term D_2 refers to the diffusion coefficient of oxygen through the ash layer, *L* denotes the total height of the heap. The term ρ denotes the porosity of the

waste heap dump. D_2 is the bulk diffusion coefficient for oxygen transport through the pore space of the heap and symbolises the particle size. The movement of the reaction front *X(t)* through the waste heap dump as a function of time is calculated with the following equation:

Equation 3.25

$$X(t) = \sqrt{2t - t_c} - \sqrt{t_c}$$

This now allows for the calculation of the oxygen profile as a function of time and can be expressed as follows:

Equation 3.26

$$u(x,t) = 1 - x\frac{\sqrt{\beta}}{\left[1 + \sqrt{\beta}X\right]} \; for\; 0 \leq x \leq X(t)$$

where $\beta = 6k$ and *x* denotes the location in the heap above the moving reaction front *X(t)*. The oxygen profile below the reaction front *X(t)* is calculated by the following equation:

Equation 3.27

$$u(x,t) = \frac{\exp(-\sqrt{\beta}(x - X))}{\left[1 + \sqrt{\beta}X\right]} \; for\; X(t) \leq x \leq 1$$

It can be shown that Equation 3.19 can be solved in PHREEQC by making use of the RATES block as discussed in the previous section. For illustration purposes a fragment of the code to model the kinetic oxidation of pyrite as described by Mayer (1999) is depicted in Figure 3.8. The following equation from the study by Mayer (1999) are modeled:

Equation 3.28

$$\frac{dr}{dt} = -10^3 S \frac{D_2}{3.5} \frac{r}{(R-r)r} [O_2]_{aq}$$

where D_2 is the diffusion coefficient of oxygen in water, r is the unreacted core radius, R is the particle radius (unreacted core plus ash layer) and S is the reactive surface and can be calculated as follows:

Equation 3.29

$$S = 3 \cdot 10^{-3} \frac{\varphi_i}{r}$$

where φ_i is the volumetric fraction of mineral at time t =t_i defined as [m^3 mineral m^{-3} bulk]. This parameter changes with time, compensating for the reduction in reaction surface as the oxidation of pyrite progresses.

Figure 3.8 shows the PHREEQC and MATLAB solutions to the equations above. The figure also shows a fragment of the PHREEQC code used to solve the equations.

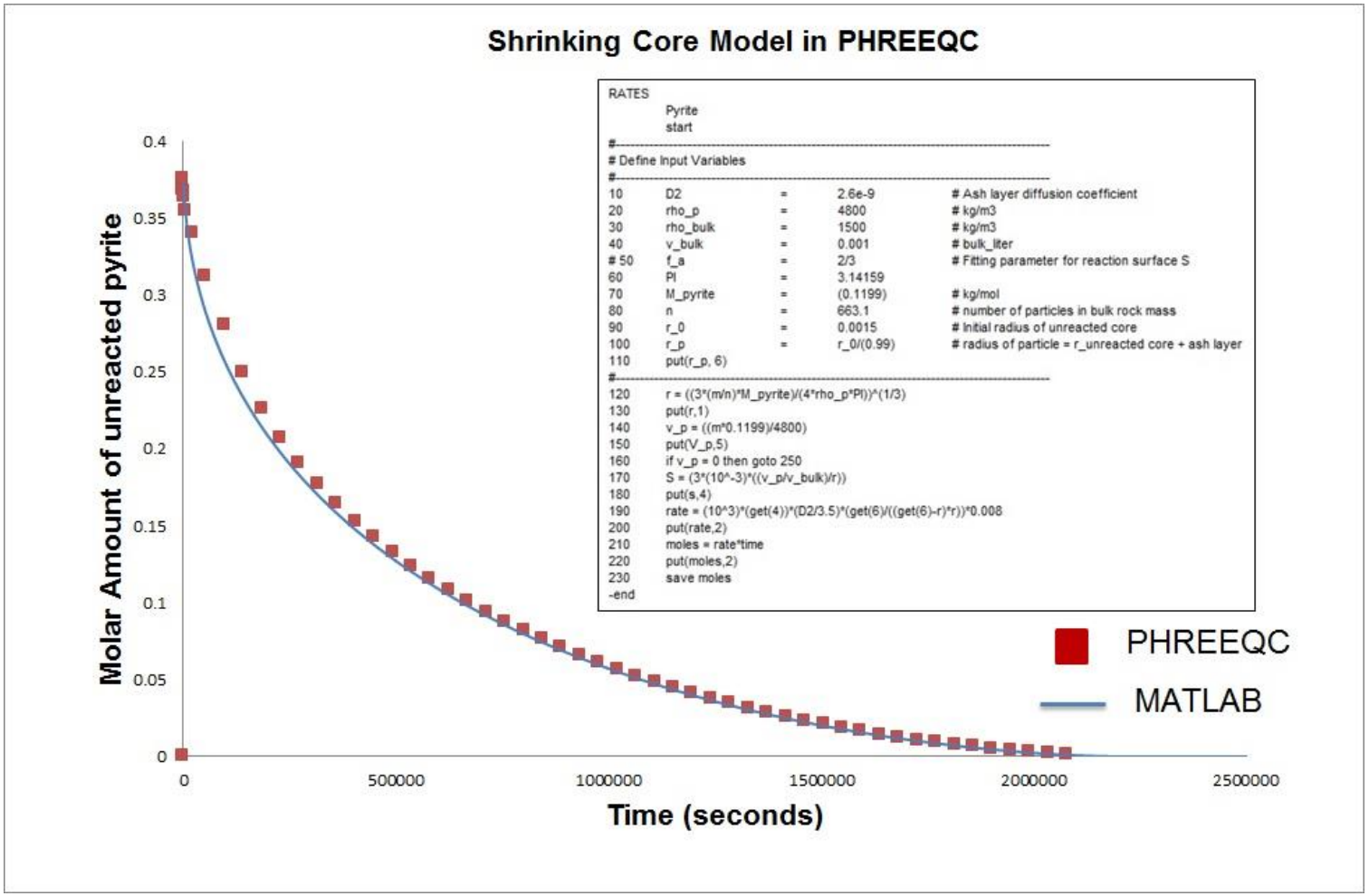

Figure 3.8: Fragment of the PHREEQC code used to calculate the oxidation rate of pyrite using the SCM kinetics

The dissolved oxygen is defined using the EQUILIBRIUM_PHASES block in PHREEQC due to the fact that PHREEQC do not have a gas transport module. For this reason it is proposed to make use of the integrated sulfide production rate proposed by Davis and Ritchie (1986a):

Equation 3.30

$$S(t) = \frac{L\delta_S k_3}{\delta} \frac{1}{\beta\sqrt{\beta}[t - (X(t)^2/2]} \cdot - \int_0^{R_t} \frac{6R^2(1-R)^2(1+2R)}{\left[(1-R)^2(1+2R)^2 - cosh^{-2}\sqrt{\beta}(1-X(t))\right]} dR$$

where L is the total height of the waste heap, δ_S is the ratio of mass of oxygen consumed per mas of sulfide generated in the pyrite oxidation reaction. The constant k_3 is calculated as follows:

Equation 3.31

$$k_3 = \frac{3\delta\rho_S k}{\tau_4}$$

where ρ_s denotes the density of pyrite in the heap and τ_4 is the characteristic time for transport. For the calculation of this constant, the reader is referred to the work done by Davis and Ritchie (1986a). For small particles it can be shown that the rate expressed in Equation 3.37 can be simplified as follows:

Equation 3.32

$$S(t) = \frac{L\delta_s\rho_s}{\tau_4} \frac{1}{\sqrt{2t - t_c}}$$

This renders an expression that is only time dependent and can be solved with ease in PHREEQC, eliminating the problem of compensating for the oxygen transport when the shrinking core model is used. The RATES block in PHREEQC will automatically integrate the rate expression when the standard procedure is used to

input a rate expression in PHREEQC. For this reason the keyword *total_time* is used to recall the current time for each time step. This value then defines the time step t in

Equation 3.32, allows the RATES block to simulate a rate expression that is only time dependent. Figure 3.9 shows the input to the rate block used to simulate the rate discussed above.

```
RATES
Pyrite
 -start
10      tau_4     = 8.96E+07
20      t1        = 0.026184797              # t_c
30      t2        = (total_time/tau_4)
31      put(t2,1)
40      t3        = t2+t1                    # t
41      put(t3,2)
50      L         = 1                        # meter
60      sig_s     = 1.616
70      rho_p     = 45



80      moles = ((L*sig_s*rho_p)/tau_4)*(1/(((2*t3)-t1)^0.5))*(1/0.12)
81      put(moles, 3)
90      save moles
-end
```

Figure 3.9: Fraction of PHREEQC code used to calculate the rate of sulphate production

3.4.3 Calculating the diffusion coefficients

The bulk diffusion coefficient D_1, governing the transport of oxygen through the pore space of the heap is a function of void space, degree of saturation of the heap and temperature. The following equation can be used to calculate the bulk diffusion coefficient (Reardon & Moddle, 1985):

Equation 3.33

$$D_1 = 3.98 \times 10^{-9} \cdot \left[\frac{\theta_A - 0.05}{0.95}\right] \cdot T^{1.5}$$

where θ_A is the air filled porosity and T denotes temperature in Kelvin.

3.4.4 Model setup

A test scenario is set up to compare results obtained from the AAS model with results obtained from PYROX. A homogenous slap with a height of 1 meter is modelled. It is assumed that the top surface area is sufficiently wide that it can be assumed that oxygen is transported from the top surface by means of diffusion as described in the previous chapters. It is assumed the particles are all spherical and identical in size with a radius of 0.001515 meter. The remaining input parameters is listed in Table 3.2, where D_2 is calculated using

Equation 3.33.

Table 3.2: Input parameters for the AAS model and PYROX simulation

Parameter		Unit	Description
L	1	m	Depth of heap
ρ	0.38		porosity
D_1	3.31E-06	m^2/s	Diffusion Coefficient of oxygen in pore space of dump
D_2	2.60E-09	m^2/s	Diffusion Coefficient of oxygen in water
a	0.001515	m	radius of particle
v	1.746		mass of oxygen used per mass of pyrite oxidized in the oxidation reaction
rs	45	kg/m^3	Density of sulphur within the dump
γ	0.03		Constant
U_0	0.265	kg/m^3	Oxygen concentration at the surface of the dump
δ	22460	J/kg	Heat produced from oxidation reaction per mass of sulphur oxidation (Davis,1983)
δs	1.616		mass ratio, not mole ratio- error

The model calculates the sulphate production on an area basis of 1 m^2 and can be conceptualized as depicted in Figure 3.10.

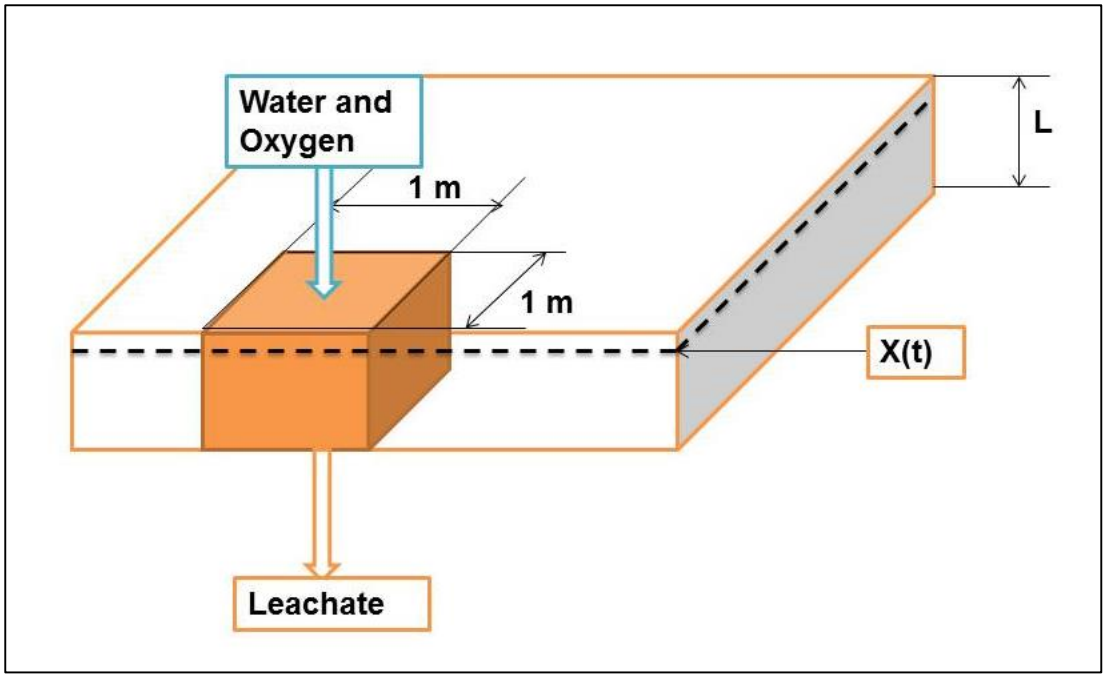

Figure 3.10: Conceptual illustration of AAS model setup

4. Model Results and Discussion

4.1 Introduction

In this chapter the results of the developed model will be presented and discussed.

4.2 Surface Kinetic model

The data obtained from the HLC were modelled by making use of the SK model. In Figure 4.1 the release of sulphates were modelled. It can be seen from the data that there is initially a very high concentration of sulphate in the leachate, this decreases exponentially over the course of the twenty week period the HCL test was conducted. The initial high value of sulphates observed can be attributed to the dissolution of gypsum and not so much to the oxidation of pyrite, for this reason gypsum was defined as a kinetic species and not as an equilibrium species. The amount of gypsum initially present was unknown, and was used as a calibration parameter to calculate the SO_4^{2-} release rate. The dissolution of gypsum is responsible for the release of SO_4^{2-} and Ca^{2+}. This complicates the calibration of the SO_4^{2-} leach rate because adjusting the amount of gypsum present also affects the Ca^{2+} release rate. Dolomite and calcite were the only two bicarbonate minerals present in the material. Both dolomite and calcite release Ca^{2+} when they dissolve. The dissolution rate of dolomite was calibrated using the Mg^{2+}, and in turn the calcite and gypsum release rates were calibrated with the SO_4^{2-} and Ca^{2+} leach data.

A reasonable model fit is obtained in the first 13 weeks, but over predicts the sulphate release thereafter. This can be attributed to the gypsum rate under predicting the speed of dissolution in the early stages of the leaching procedure as it is anticipated that the initial gypsum present in the system would have leached out in the first two to three weeks.

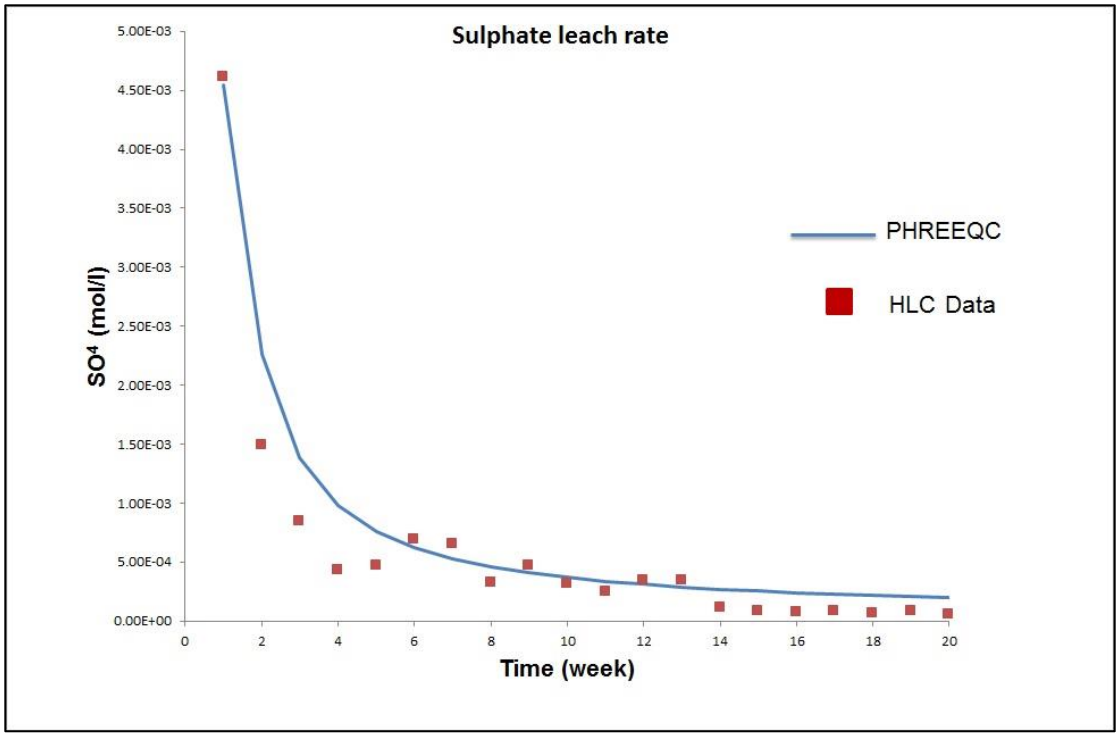

Figure 4.1: Sulphate leach rate calculated by the SK model compared to HLC data

Figure 4.2 show the leach rate of Ca^{2+} predicted by the surface kinetic model compared to HLC data. It can be seen that the model does not adequately predict the release of calcium in the first 13 weeks. The over prediction from the model in the first 8 weeks may be attributed to the contribution of gypsum.

Figure 4.3 show the release rate of Mg^{2+} calculated by PHREEQ compared to HLC data. The figure show a similar trend to that of Figure 4.2 suggesting that the dolomite rate law may not be adequate in describing the dissolution of dolomite. This may be contributed to the over prediction of calcium in the system.

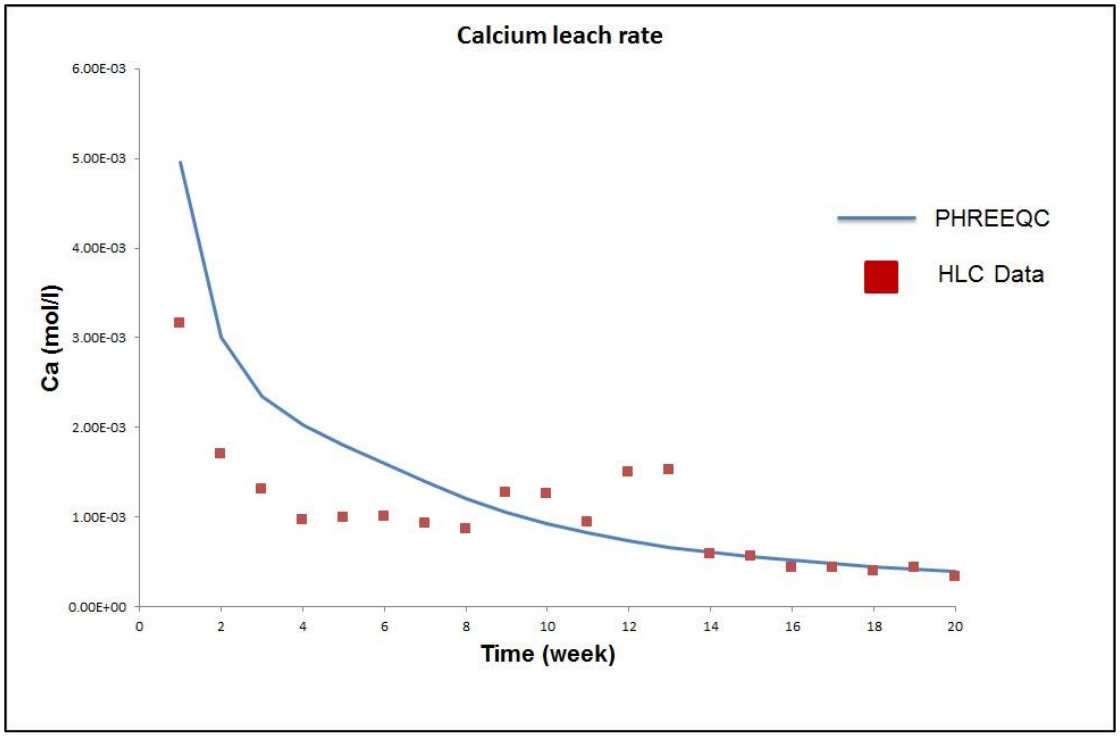

Figure 4.2: Calcium leach concentrations calculated by the SK model compared to HLC data

The almost sinusoidal oscillation of the leach data observed in all the parameters described above can be attributed to the leach test procedure with the cycling of dry and moist air and leaching with water only once a week. The PHREEQC model does not take this behaviour into account and thus explains the deviation of the model with the HLC data at weeks 6-7 and weeks 12-13.

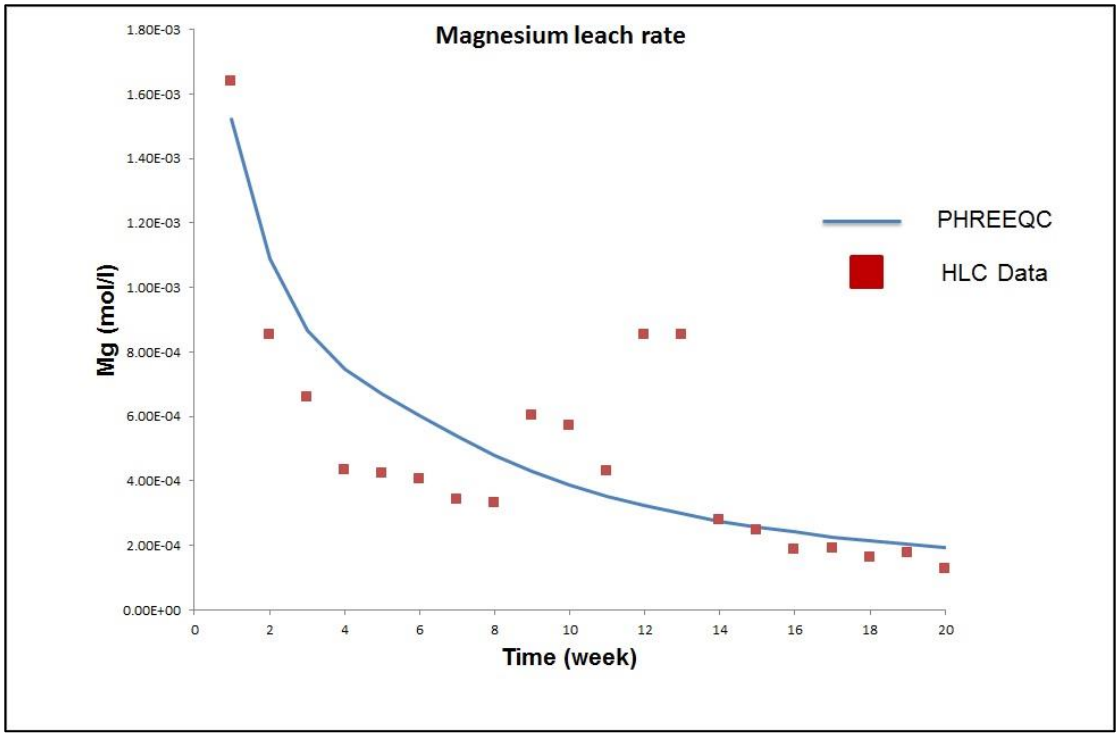

Figure 4.3: Magnesium leach concentration calculated by the SK model compared to HLC data

4.3 Up-Scaling to field conditions

4.3.1 Oxygen transport

Figure 4.4 below depicts the movement of the planar reaction from the top surface of the heap through the length of the heap as a function of time. The Approximate Analytical Solution is used to calculate the movement through the heap, the results from this model is compared to the results obtained from PYROX for the same conditions.

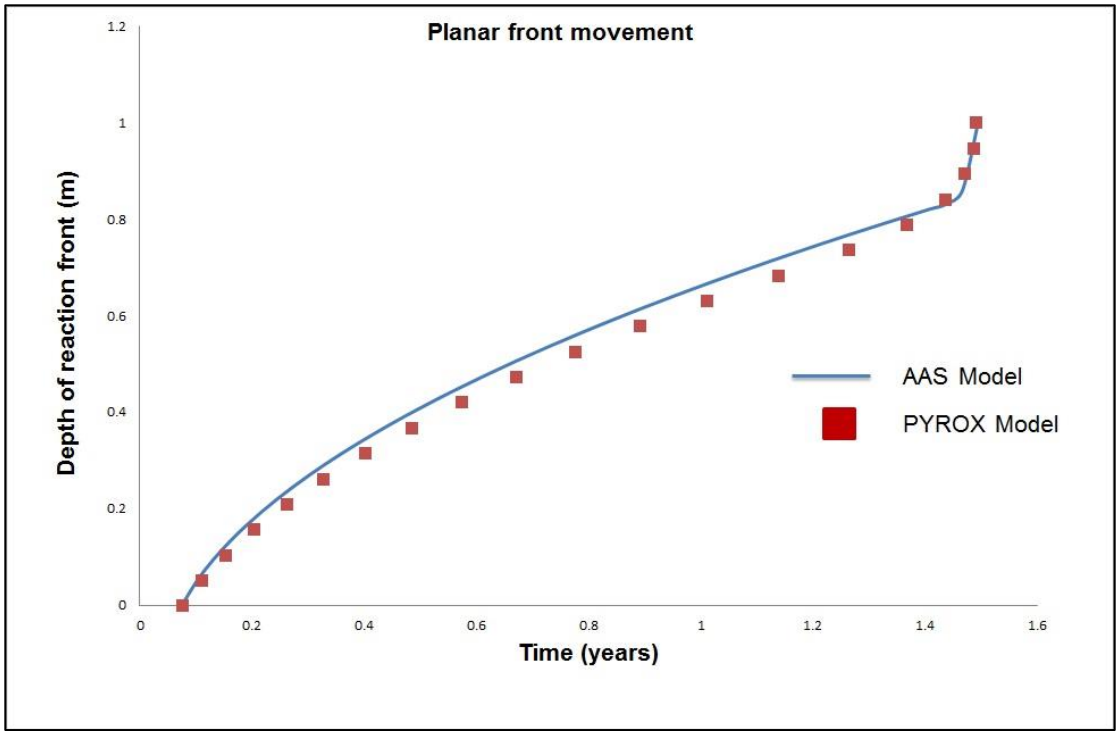

Figure 4.4: Planar front movement through the heap as a function of time: AAS model compared to the PYROX model

Figure 4.5 shows the oxygen profiles as a function of time as calculated by Equation 3.25 and Equation 3.26. This result is compared to results obtained from PYROX.

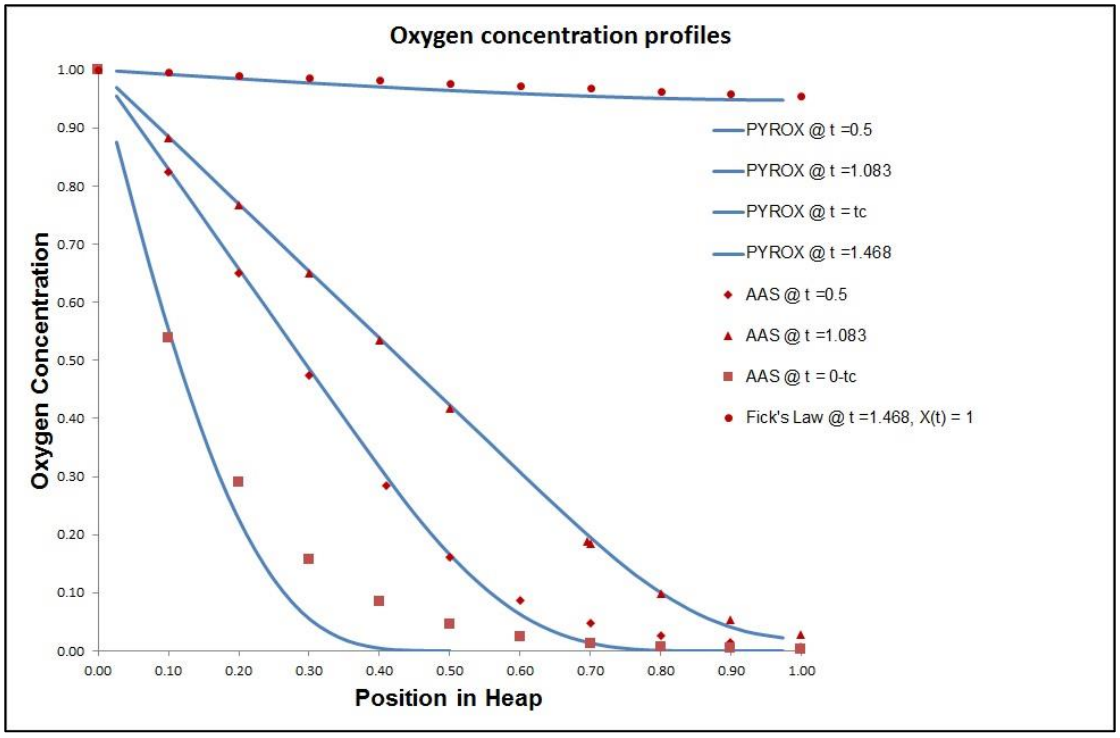

Figure 4.5: Oxygen concentration profiles for various time intervals throughout the lifetime of the heap

Figure 4.6 shows the integrated sulphate production rate of sulphate compared to the integrated sulphate production rate calculated by PYROX for the same conditions. It can be seen from Figure 4.4 that in the initial stage of the simulation the AAS model over predicts the pore space oxygen concentration. This effect can also be observed in Figure 4.4. The over prediction of oxygen is directly linked to the under prediction in sulphate production rate, as the pyrite is not oxidizing as fast in the initial stages of the AAS model compared to the PYROX model. The AAS model predicts the time for the heap to be fully oxidized to take around one and a half years, the same as PYROX.

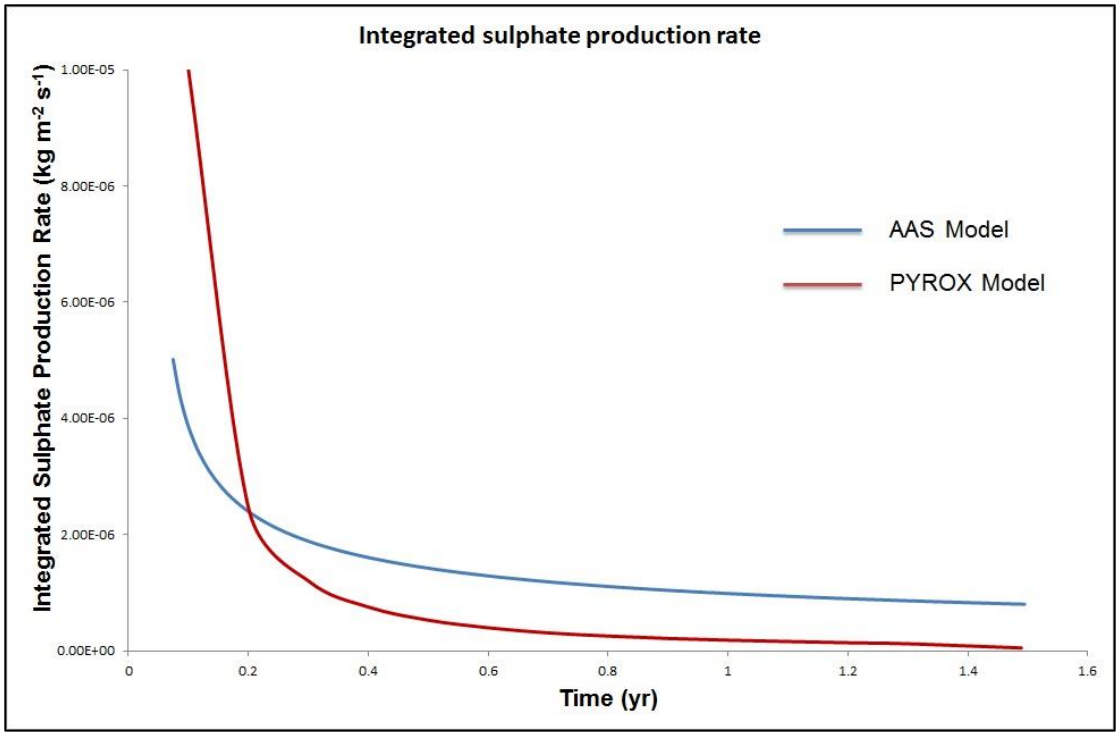

Figure 4.6: The integrated sulphate production rate calculated by the AAS model compared to the results obtained from PYROX

5. Conclusions and Recommendations

It was shown in this study that PHREEQC can be used to develop a reasonable model to describe the leach behaviour of a HLC. The results obtained from the model were compared with data obtained from a standard humidity leach cell as outlined by Usher *et al*. (2002). Reaction kinetics obtained from literature was used to describe the reactions anticipated in the HLC and was found to describe the trends observed in the HCL data to a reasonable extent.

Deviations of the model from observed data was attributed to the possible presence of gypsum in the system. This caused complications in describing the release of magnesium and calcium. The kinetic rate law used to describe the dissolution of dolomite was also simplified. This may have introducing a possible error into the model.

It was seen from literature that diffusive oxygen transport into a waste heap dump is in most cases the rate determining step in the acid generation of a waste heap dump. Several mathematical models were identified that describe this behaviour. An analytical approach (AAS model) developed by Davis (1983) was used to model the oxygen transport to the reaction sites in the heap and the subsequent production of sulphates. The results obtained from this model were compared to the results obtained from PYROX. It was shown that the integrated sulphate production rate obtained from the AAS model can be modelled in PHREEQC. This provides then a usable model that can be applied to model waste heap dump scenarios.

It was found from the modelling results and comparison with PYROX that the model under predicts the integrated sulphate production rate in the initial stages of the reacting waste heap dump. It does however show results that are in close agreement with the results obtained from PYROX in later stages of the lifespan of the waste heap dump. This provides then limitations to the AAS model's applicability on geochemical problems. The model can only be applied to describe waste heap dumps where the particles at the top of the heap are fully oxidized.

Several shortfalls were identified during the development of the model; the most prominent problems will be listed below with recommendations to address these issues:

- Reaction rate laws found in literature may not adequately describe the kinetic dissolution of minerals. This may introduce errors in the model when the kinetic rate laws are calibrated to fit the data. It is therefore recommended additional XRD tests be conducted of the HLC sample on completion of the leach test in order to perform a mass balance to validate the calibrated reaction kinetic rate laws in terms of conversion of the dissolution reaction.
- It is assumed in this work that a HLC can be approximated by a CSTR reactor model. This may be an over simplification as the CSTR approach assumes the system is well mixed and do not account for stagnant zones in the system. This may be rectified by making uses of a reactor in series approach to account for stagnant zones.

6. References

AKCIL, A. & KOLDAS, S. 2006. Acid Mine Drainage (AMD): causes, treatment and case studies. Journal of Cleaner Production 14:1139-1145.

ANDRE, B.J. 2009. Generation of acid mine drainage: reactive transport models incorporating geochemical and microbial kinetics, PhD thesis: University Of Colorado At Boulder.

APPELO, C. A., VERWEIJ, J.E. & SCHAFER, H. 1998. A hydrogeochemical transport model for an oxidation experiment with pyrite/calcite/exchangers/organic matter containing sand. Appl. Geochem., 13:257–268.

APPELO, C.A.J. & POSTMA, D. 2005. Geochemistry, groundwater and pollution. Boca Raton: CRC Press.

ARDEJANI, F. D., SHOKRI, B.J., MORADZADEH, A., SOLEIMANI, E. & JAFARI, M.A. 2008. A combined mathematical geophysical model for prediction of pyrite oxidation and pollutant leaching associated with a coal washing waste dump. Int. J. Environ. Sci. Tech., 5 (4):517-526.

ASTM. 2001. Standard test method for accelerated weathering of solid materials using a modified Humidity Cell, D 5744-96ASTM (2007) Standard test method for laboratory weathering of solid materials using a humidity cell, D5744-07, pp. 1–19.

BAIN, J.G., MAYER, K.U., BLOWES, D.W., FRIND, E.O., MOLSON, J.W.H., KAHNT, R. & JENK, U. 2001. Modelling the closure-related geochemical evolution of groundwater at a former uranium mine. Journal of Contaminant Hydrology 52,109–135.

BANWART, S.A. & MALMSTRÖM, M.E. 2001. Hydrochemical modelling of preliminary assessment of mine water pollution. Journal of Geochemical Exploration 74, 73-97

BERGER, A.C., BETHKE, C.M. & KRUMHANSL, J.L. 2000. A process model of natural attenuation in drainage from a historic mining district. Applied Geochemistry 15:655-666.

BETHKE C.M., 2008. Geochemical and Biogeochemical Reaction Modeling. Cambridge University Press, 547 pp.

BROWN, P., LUO, X.L., MOONEY, J. & PANTELIS, G. 1999. The modelling of flow and chemical reactions in waste piles. In: 2nd Internat. Conf. CFD in the Minerals and Process Industries. CSIRO, Melbourne, Australia, December 6–8, pp. 169-174.

BROWN, J.G., PIERRE D. & GLYNN, P.D. 2003. Kinetic dissolution of carbonates and Mn oxides in acidic water: measurement of in situ field rates and reactive transport modelling. Applied Geochemistry 18:1225–1239.

COLLON, P., FABRIOL, R. & BUÈS, M. 2006. Modelling the evolution of water quality in abandoned mines of the Lorraine Iron Basin. Journal of Hydrology, vol. 328, pp 620– 634.

DAVIS, G.B. & RITCHIE, A.I.M. 1986(a). A model of oxidation in pyritic mine waste: part 1: equations and approximate solution, Applied Mathematical. Modelling, vol. 10, pp. 314–322.

DAVIS, G.B. & RITCHIE, A.I.M. 1986(b). A model of oxidation in pyritic mine waste: part 2: comparison of numerical and approximate solution, Applied Mathematical. Modelling, vol. 10, pp. 314–322.

DAVIS, G.B. & RITCHIE, A.I.M. 1986(c). A model of oxidation in pyritic mine waste: part 3: import of particle size distribution, Applied Mathematical. Modelling, vol. 10, pp. 314–322.

DAVIS, G.B. 1983. Mathematical modelling of rate-limiting mechanisms of pyritic oxidation in overburden dumps, PhD thesis: The University of Wollongong.

EVANGELOU. V.P. 1995. Pyrite Oxidation and it's Control: solution chemistry, surface chemistry, acid mine drainage (AMD), molecular oxidation mechanisms, microbial role, kinetics, control, ameliorates and limitations, microencapsulation. 1st ed. CRC Press.

GERKE, H.H., MOLSON, J.W. & FRIND, E.O. 2001. Modelling the impact of physical and chemical heterogeneity on solute leaching in pyritic overburden mine spoils. Ecological Engineering 17: 91–101.

KORETSKY, M.D. 2003. Engineering and Chemical Thermodynamics, USA: John Wiley & Sons.

LEFEBVRE, R., HOCLLEY, D., SMOLENSKY, J. & GÉLINAS, P. 2001. Multiple transfer processes in waste rock piles producing acid mine drainage 1: Conceptual model and system characterization. Journal of Contaminant Hydrology 52: 137-164.

LEVENSPIEL, O. 1999. Chemical Reaction Engineering. 3d ed. New York: Wiley.

LINKLATER, C.M., SINCLAIR, D.J. & BROWN, P.L. 2005. Coupled chemistry and transport modelling of sulphidic waste rock dumps at the Aitik mine site, Sweden. Applied Geochemistry 20:275–293.

MAYER, U. K. 1999. A numerical model for multicomponent reactive transport in variably saturated porous media. Ph.D. Thesis, Dept. of Earth Sciences, University of Waterloo, Waterloo, Ontario, Canada.

MAYER, U.K., FRIND, E. O. & BLOWES, D.W. 2002. Multicomponent reactive transport modeling in variably saturated porous media using a generalized formulation for kinetically controlled reactions. Water Resources Research, vol. 38.

MILLER, S., ROBERTSON, A. & DONAHUE, T. 1997. Advances in acid drainage prediction using the net acid generation (NAG) 4th international conference on acid rock drainage.

MOLSON, J.W., FALA, O., AUBERTIN, M. & BUSSIÈRE, B. 2005. Numerical simulations of pyrite oxidation and acid mine drainage in unsaturated waste rock piles. Journal of Contaminant Hydrology 78:343-371.

MOLSON, J., FALA, O., AUBERTIN, M. & BUSSIÈRE, B. 2008. Geochemical transport modelling of acid mine drainage within heterogeneous waste rock piles. In Proceedings of the 61 st Canadian Geotechnical Conference and 9th Joint CSG/IAHCNC Groundwater Specialty Conference, Edmonton, Alta., 21-24 September 2008. BiTech Publishers Ltd., Richmond, B.C. pp. 1586-1593.

MORIN, K.A., CHERRY, J.A., DAVE, N.K., LIM, T.P. & VIVYURKA, A.J. 1987. Migration of acidic groundwater seepage from uranium-tailings impoundments: 1. Field study and conceptual hydrogeochemical model. Journal of Contaminant Hydrology 2: 217–303.

NICHOLSON, R.V., RINKER, M.J., ACOTT, G. & VENHUIS, M.A. 2003. Integration of field data and a geochemical transport model to assess mitigation strategies for an acid-generating mine rock pile at a uranium mine. Proceedings, Sudbury: Mining and the Environment.

NORDSTROM, D.K. 2010. Advances in the Hydrogeochemistry and Microbiology of Acid Mine Waters. International Geology Review 42:6, 499-515.

PANTELIS, G., RITCHIE, A.I.M. & STEPANYANTS, Y.A. 2001. A conceptual model for the description of oxidation and transport processes in sulphidic waste rock dumps. Applied Mathematical Modelling 26: 751-770.

PARKHURST, D.L. & APPELO, C.A.J. 2003. User's guide to PHREEQC (version 2)— a computer program for speciation, batch-reaction, one-dimensional transport, and inverse geochemical calculations. Report 99-4259. US Geological Survey Water-Resources Investigations.

POKROVSKY, O.S., GOLUBEV, S.V., SCHOTT, J. & CASTILLO, A. 2009. Calcite, dolomite and magnesite dissolution kinetics in aqueous solutions at acid to circumneutral pH, 25 to 150 °C and 1 to 55 atm pCO2: New constraints on CO2 sequestration in sedimentary basins. Chem. Geo., 265:20–32.

PRICE, W.A. 1997. Guidelines and recommended methods for the prediction of metal leaching and acid rock drainage at minesites in British Columbia (DRAFT). British Columbia Ministry of Employment and Investment, Energy and Minerals Division, Smithers: BC, pp.143.

REARDON, E.J. & MODDLE, P.M., 1985. Gas diffusion coefficient measurements on uranium mill tailings: Implications to cover layer design. Uranium 2: 111–131.

SKOUSEN, J., SIMMONS, J., MCDONALD, L. M. & ZIEMKIEWICZ, P. 2002. Acid–Base Accounting to Predict Post-Mining Drainage Quality on Surface Mines. J. Environ. Qual. 31:2034–2044.

STRÖMBERG, B. & BANWART, S.1999. Weathering kinetics of waste rock from the Aitik copper mine, Sweden: scale dependent rate factors and pH controls in large column experiments. Journal of Contaminant Hydrology 39: 59–89.

SUNKAVALLI, S.P. 2014. Gap between Humidity Cell Testing Data and Geochemical Modeling of Acid Rock Drainage. ISSN: 2157-7587 HYCR, an open access journal.

TIRUTA-BARNA, L., RAKOTOARISOA, Z. & MEHU, J., 2006. Assessment of the multi-scale leaching behaviour of compacted coal fly ash. J. Hazard. Mater. 137:1466–147.

TIRUTA-BARNA, L. 2008. Using PHREEQC for modelling and simulation of dynamic leaching tests and scenarios. Journal of Hazardous Materials 157:525–533.

USHER, B.H., CRUYWAGEN, L-M., DE NECKER, E. & HODGSON, F.D.I. 2002. On-site and laboratory investigations of spoil in opencast collieries and the development of acid-base accounting procedures, Water Research Commission.

WUNDERLEY, M.D., BLOWES, D.W., FRIND, E.O., PTACEK. C.J. & AL, T.A. 1995. A Multicomponent reactive transport model incorporating kinetically controlled pyrite oxidation. Convergence on Mining and the Environment, Sudbury, Ontario.

WUNDERLEY, M.D. & BLOWES, D.W. 1997. PYROX version 1.1 User Manual. Institute for Groundwater Research, Unvi. Of Waterloo, Waterloo, Ontario.

YOUNGER, P. 2000. Predicting Temporal changes in total iron concentrations in groundwater flowing from abandoned deep mines: a first approximation. Journal of Contaminant Hydrology 44 : 47–69.

ZHANG, R., HU, S., ZHANG, X. & YU, W. 2007. Dissolution Kinetics of Dolomite in Water at Elevated Temperatures. Aquat Geochem 13:309–338.

Appendix A: Mineralogy

INTRODUCTION

The mineralogical composition of the rock samples was determined by means of X-ray Diffraction (XRD). The XRD was performed at Waterlab (PTY) Ltd, Pretoria. The total element analyses were performed by means of X-ray Fluorescence (XRF) at the Council for Geoscience, Pretoria.

METHODOLOGY

The material was prepared for XRD analysis using a backloading preparation method. It was analysed with a PANalytical Empyrean diffractometer with PIXcel detector and fixed slits with Fe filtered Co-Kα radiation. The phases were identified using X'Pert Highscore plus software;

The relative phase amounts (weight%) were estimated using the Rietveld method. Errors are on the 3 sigma level in the column to the right of the amount (in weight per cent).

RESULTS

The results of the XRD and XRF are listed below in Table A-1, Table A-2 and Table A-3 respectively.

Table A-1: XRD results (weight % with error)

Composition (%) [s]		
Sample 1		
Mineral	Amount (weight %)	Error
Anatase	5.45	0.45
Calcite	6.22	0.72
Dolomite	15.17	1.17
Kaolinite	61.6	1.35
Pyrite	5.43	0.6
Quartz	6.13	0.6

Table A-2: XRF major elements (weight %)

Trace Elements	Trace Element Concentration
	Sample 1
U	2.36
V	54
W	1.39
Y	22.5
Yb	3.7
Zn	37
Zr	118
As	<5.00
Ba	88
Bi	<5.00
Br	<1.00
Cd	<5.00
Ce	<5.00
Cl	327
Co	17.1
Cs	<1.00
Cu	36.1
Ga	14.1
Ge	<1.00
Hf	2.81
Hg	<5.00
La	17.9
Lu	<1.00
Mo	3.32
Nb	9
Nd	21.1
Ni	37
Pb	<5.00
Rb	18.5
Sb	<5.00
Sc	6.2
Se	<1.00
Sm	3.15
Sn	<5.00
Sr	156
Ta	1.23
Te	2.96
Th	11.1
Tl	<1.00

Table A-3: XRF trace element concentration (ppm)

Trace Elements	Trace Element Concentration
	Sample 1
U	2.36
V	54
W	1.39
Y	22.5
Yb	3.7
Zn	37
Zr	118

Appendix B: Static Procedures

INTRODUCTION

Acid base accounting (ABA) is a valuable and widely used static test that determines both the acid-generating and acid neutralizing potential of a sample. A description of the different ABA components is given below:

Acid potential (AP) is determined by the % S with a factor of 31.25. The units of AP is kg CaCO3/t rock and indicates the theoretical amount of calcite that would be required to neutralize the acid produced; and

The Neutralization Potential (NP) is determined by reacting the sample with a known excess of standardized hydrochloric or sulphuric acid. The paste is then back titrated with standardized sodium hydroxide. This is done to determine the unconsumed acid. NP is also expressed as kg CaCO3/t rock.

Net Neutralization Potential (NNP) is determined by subtracting AP from NP. NNP is used to screen the ABA results in terms of their ARD potential. The criteria are as follows:

If NNP = NP – AP < 0 The sample has the potential to generate acid

If NN = NP – AP > 0 The sample has the potential to neutralise acid

Research have shown that a range of values for NNP between -20 to 20 kg/t CO_3 can either become acidic or neutral, and is therefore uncertain (Usher *et al.*, 2002).

Neutralising Potential Ratio (NPR) is the NP: AP ratio. Guidelines for screening criteria based on the ABA results are listed below in Table B-1.

Table B-1: Screening methods using NPR (Price, 1997)

Potential to generate Acid Rock Drainage	NPR	Comments
Rock Type I: Likely	<1:1	Likely to generate ARD
Rock Type II: Possibly	1:1-2:1	Possible ARD generating
Rock Type III: Low	2:1-4:1	Possibly AMD generating if NP is insufficiently reactive or is depleted at a faster rate than sulphides.
Rock Type IV: None	>4:1	No further AMD testing required unless materials are to be used as a source of alkalinity.

% S and NPR

From Table B-1 and %S from the ABA (Leco) results a graph can be plotted to visually represent the ABA results. Samples with %S content of less than 0.3% is regarded as having insufficient oxidisable %S and will not sustain acid generation. Samples with a NRP value above 4 is considered to have enough neutralisation capacity to be classified to have a very low probability to produce acid. Samples with a NRP value of lower than 1 and a %S content that exceed 0.3% are regarded as highly probable of producing acid.

NAG test terminology and screening methods

The Net acid Generating (NAG) test consists of rapidly oxidizing sulphide minerals in a sample using hydrogen peroxide (H_2O_2). This value can serve as a rough guideline to assess the potential of a material to produce acid after a period of weathering. It should be noted that this represents a worst case scenario where all the sulphide minerals are reacted completely. This will not be the case under field conditions, as sulphide minerals are shielded in the rock matrix. Several other factor also control the rate of sulphide mineral oxidation, causing a slower release of sulphide oxidation products than what is observed in peroxide extraction. It is assumed with these tests that the elevation of SO_4 is a direct result of the sulphide mineral oxidation. The methodology is described by Usher *et al.* (2002). The potential of the sample to generate acidic drainage is calculated as the difference

Table B-2: Screening criteria for NAG test

Final pH in NAG Test	Acid Generating Potential
>5.5	Non-acid generating
3.5-5.5	Low risk acid generating
<3.5	High risk acid generating

Appendix C: Leach Test Data

Chemical Parameter (mg/l)	WEEK																			
	1	2	3	4	5	6	7	8	9	10	11	12	13	14	15	16	17	18	19	20
pH	7.35	7.69	7.74	8.24	8.11	8.49	8.51	8.31	8.04	8.07	8.06	7.87	7.88	8.04	8.05	8.00	8.00	8.01	7.96	8.02
Electrical Conductivity (mS/m)	97.9	54.3	42.0	30.6	31.0	33.6	32.0	26.4	27.1	22.9	21.1	25.3	24.0	17.1	14.4	12.5	12.9	11.0	11.9	8.9
Total Dissolved Solids	669	365	291	210	214	229	218	182	186	159	146	172	166	120	100	88	92	74	80	62
Total Alkalinity as $CaCO_3$	120	140	148	120	108	136	136	108	104	100	108	136	138	83	65	60	60	53	55	46
Ammonia-N	0.3	<0.2	0.2	<0.2	<0.2	<0.2	<0.2	<0.2	0.2	<0.2	<0.2	<0.2	<0.2	<0.2	<0.2	<0.2	<0.2	<0.2	<0.2	<0.2
Nitrate-N	<0.2	<0.2	<0.2	<0.2	<0.2	<0.2	<0.2	<0.2	<0.2	<0.2	<0.2	<0.2	<0.2	<0.2	<0.2	<0.2	<0.2	<0.2	<0.2	<0.2
Chloride-Cl	<0.2	<0.2	<0.2	<0.2	<0.2	<0.2	<0.2	<0.2	<0.2	<0.2	<0.2	<0.2	<0.2	<0.2	<0.2	<0.2	<0.2	<0.2	<0.2	<0.2
Sulphate-SO_4	443	143	81	41	45	66	63	31	45	30	24	33	33	11	8	7	8	6	8	<5
Fluoride-F	<0.2	0.2	0.2	0.2	0.2	0.2	0.2	0.2	<0.2	<0.2	<0.2	0.4	0.4	0.4	0.4	0.4	0.4	0.4	0.4	0.4

ICP-MS Scan (mg/l)	WEEK																			
	1	2	3	4	5	6	7	8	9	10	11	12	13	14	15	16	17	18	19	20
Silver-Ag	0.001	0.000	0.000	0.001	0.000	0.000	0.000	0.000	0.000	0.000	0.000	0.000	0.000	0.000	0.000	0.000	0.000	0.000	0.000	0.000
Aluminium-Al	0.134	0.108	0.099	0.091	0.091	0.086	0.088	0.082	0.102	0.106	0.089	0.104	0.106	0.062	0.063	0.056	0.054	0.050	0.055	0.047
Arsenic-As	0.000	0.000	0.000	0.001	0.002	0.001	0.000	0.000	0.001	0.000	0.000	0.000	0.000	0.000	0.000	0.000	0.000	0.000	0.000	0.000
Boron-B	0.383	0.350	0.297	0.228	0.199	0.178	0.169	0.172	0.208	0.169	0.105	0.092	0.087	0.051	0.047	0.034	0.034	0.029	0.027	0.019
Barium-Ba	0.250	0.202	0.140	0.157	0.155	0.141	0.136	0.131	0.131	0.124	0.116	0.061	0.062	0.133	0.210	0.173	0.222	0.220	0.252	0.231
Beryllium-Be	0.000	0.001	0.000	0.000	0.001	0.000	0.000	0.000	0.000	0.000	0.000	0.001	0.000	0.000	0.000	0.001	0.000	0.001	0.001	0.000
Bismuth-Bi	0.000	0.000	0.000	0.000	0.000	0.000	0.000	0.000	0.000	0.000	0.000	0.002	0.003	0.003	0.000	0.002	0.000	0.000	0.001	0.003
Calcium-Ca	126.6	68.03	52.60	38.51	39.60	40.30	37.40	34.80	51.04	50.56	37.59	59.99	61.12	23.71	22.37	17.13	17.38	15.89	17.28	13.14
Cadmium-Cd	0.000	0.000	0.000	0.000	0.000	0.000	0.000	0.000	0.000	0.000	0.000	0.000	0.000	0.000	0.000	0.001	0.000	0.001	0.001	0.000
Cobalt-Co	0.004	0.000	0.000	0.000	0.000	0.000	0.000	0.000	0.000	0.000	0.000	0.000	0.000	0.000	0.000	0.001	0.000	0.000	0.000	0.000
Chromium-Cr	0.000	0.000	0.000	0.000	0.000	0.000	0.000	0.000	0.000	0.000	0.000	0.000	0.000	0.000	0.000	0.000	0.000	0.000	0.000	0.000
Copper-Cu	0.003	0.000	0.000	0.000	0.000	0.000	0.000	0.000	0.000	0.000	0.000	0.000	0.000	0.000	0.000	0.000	0.000	0.000	0.000	0.000
Iron-Fe	0.076	0.021	0.021	0.010	0.061	0.044	0.036	0.029	0.012	0.009	0.006	0.005	0.024	0.010	0.002	0.002	0.004	0.003	0.007	0.003
Potassium-K	9.524	6.839	5.107	3.960	3.470	3.286	3.140	3.076	3.980	3.868	2.374	3.314	3.337	1.198	0.852	0.682	0.653	0.563	0.520	0.429
Lithium-Li	0.000	0.000	0.000	0.000	0.000	0.000	0.000	0.000	0.000	0.000	0.000	0.018	0.018	0.000	0.017	0.017	0.018	0.019	0.019	0.000
Magnesium-Mg	39.85	20.71	15.97	10.53	10.24	9.860	8.340	8.070	14.67	13.88	10.42	20.73	20.74	6.749	6.013	4.574	4.626	3.952	4.299	3.084
Manganese-Mn	0.255	0.104	0.077	0.061	0.066	0.071	0.063	0.059	0.082	0.081	0.058	0.050	0.049	0.023	0.020	0.012	0.010	0.008	0.008	0.005

ICP-MS Scan (mg/l)	WEEK																			
	1	2	3	4	5	6	7	8	9	10	11	12	13	14	15	16	17	18	19	20
Molybdenum-Mo	0.003	0.004	0.004	0.004	0.004	0.002	0.003	0.004	0.003	0.002	0.002	0.001	0.001	0.001	0.000	0.000	0.001	0.000	0.001	0.001
Sodium-Na	7.512	5.085	4.101	2.698	2.314	2.106	2.077	1.894	3.330	3.082	1.791	2.955	3.068	0.911	0.726	0.547	0.635	0.495	0.633	0.379
Nickel-Ni	0.046	0.071	0.027	0.013	0.015	0.011	0.009	0.012	0.025	0.037	0.025	0.034	0.036	0.006	0.007	0.004	0.003	0.002	0.001	0.001
Phosphorous-P	0.025	0.012	0.003	0.007	0.018	0.012	0.017	0.011	0.000	0.003	0.005	0.007	0.004	0.000	0.009	0.000	0.004	0.000	0.000	0.006
Lead-Pb	0.000	0.000	0.000	0.000	0.000	0.000	0.000	0.000	0.001	0.000	0.001	0.006	0.003	0.005	0.003	0.002	0.004	0.002	0.002	0.002
Sulphur-S	162.9	54.37	28.44	14.49	16.61	19.48	18.82	14.60	53.12	51.65	31.29	40.11	40.14	5.761	6.310	4.404	4.661	3.979	4.733	2.952
Antimony-Sb	0.004	0.010	0.008	0.002	0.006	0.004	0.002	0.002	0.000	0.000	0.000	0.001	0.002	0.002	0.002	0.000	0.000	0.000	0.000	0.000
Selenium-Se	0.002	0.000	0.000	0.000	0.000	0.000	0.000	0.000	0.001	0.000	0.000	0.000	0.001	0.001	0.002	0.002	0.001	0.002	0.002	0.001
Silicon-Si	1.293	1.357	1.254	0.960	0.949	0.881	0.869	0.749	1.084	1.028	0.643	0.810	0.790	0.290	0.295	0.209	0.209	0.180	0.199	0.144
Tin-Sn	0.000	0.000	0.000	0.006	0.000	0.001	0.000	0.001	0.000	0.000	0.000	0.010	0.012	0.013	0.003	0.010	0.009	0.017	0.019	0.015
Stronsium-Sr	0.724	0.392	0.377	0.313	0.320	0.334	0.306	0.298	0.367	0.368	0.278	0.329	0.322	0.156	0.162	0.128	0.137	0.124	0.132	0.098
Titanium-Ti	0.032	0.012	0.002	0.004	0.019	0.011	0.077	0.010	0.017	0.028	0.016	0.004	0.000	0.000	0.007	0.015	0.013	0.009	0.005	0.002
Thallium-Tl	0.000	0.000	0.000	0.000	0.000	0.000	0.000	0.000	0.000	0.000	0.000	0.000	0.000	0.000	0.000	0.000	0.000	0.000	0.002	0.000
Vanadium-V	0.000	0.001	0.000	0.001	0.000	0.000	0.000	0.000	0.000	0.000	0.000	0.000	0.000	0.000	0.000	0.000	0.000	0.000	0.000	0.000
Wolfram-W	0.000	0.000	0.000	0.000	0.000	0.000	0.000	0.000	0.000	0.000	0.000	0.003	0.002	0.000	0.000	0.003	0.002	0.001	0.003	0.002
Zinc-Zn	0.064	0.054	0.037	0.022	0.054	0.048	0.042	0.040	0.039	0.019	0.088	0.033	0.033	0.017	0.024	0.013	0.012	0.011	0.010	0.008
Zirconium-Zr	0.000	0.000	0.000	0.000	0.000	0.000	0.000	0.000	0.000	0.000	0.000	0.000	0.000	0.000	0.000	0.000	0.000	0.000	0.000	0.000

Appendix D: PHREEQC Code

CSTR function:

```
TRANSPORT
-cells 1; -boundary_conditions constant closed; -flow_direction diffusion_only
-stagnant 1       # 1 stagnant layer, but more are possible, for modeling bad mixing in the tank

-time_step 144 hour              # each time_step, the MIX is performed
-shifts 20                       # number of time_steps, total time is 100 hours
-punch_cells 3                   # only graph the tank solution
-punch_frequency 1               # sample every 5 hours
```

Rates:

```
RATES
Pyrite
  -start
1      A = 2* m0 # initial moles of the kinetic reactant ( initial surface per mole of pyrite (m2/mol pyrite))
2      V = 0.75
10     if SI("Pyrite")> 0 then goto 100
20     fH = mol("H+")
30     fFe2 = (1 + tot("Fe(2)")/1e-6)
# 40   if mol("O2") < 1e-6 then goto 80
50     rO2 = 10^-8.3 * mol("O2")^0.5 * fH^-0.11
90     rate = A/V * (m/m0)^ 5* rO2 * (1-SR("Pyrite")) # The shrinking reactive surface seems to control the reaction rate, as the rate is much faster when published values for n is used. A very large exponential factor for (m/m0) is requiered to fit the data
100    save rate * time
 -end

# Gypsum
# -start
# 1    A  = 4 *m0
# 2    V  = 0.75
# 10   rate = (A/V)*(m/m0)^6* 5.8*10^-7.6*(1-SR("Gypsum"))
# 20   save   rate*time
# -end
Dolomite
```

```
 -start
  1 A = 20*m0
  2 V = 0.75
  10 rate = (10^-10 )* (1 -  SR("Dolomite"))*((m/m0)^30)*((A/V))
  20 save rate * time
 -end
```

Kinetics:

```
KINETICS 3
Pyrite; -m0 0.045
# Gypsum; -m0 0.018
Dolomite;-m0  0.82
```